

# The transfer matrix: a geometrical perspective

Luis L. Sánchez-Soto<sup>a</sup>, Juan J. Monzón<sup>a</sup>, Alberto G. Barriuso<sup>a</sup>, José F. Cariñena<sup>b</sup>

<sup>a</sup>*Departamento de Óptica, Facultad de Física, Universidad Complutense, 28040 Madrid, Spain*

<sup>b</sup>*Departamento de Física Teórica, Facultad de Ciencias, Universidad de Zaragoza, 50009 Zaragoza, Spain*

---

## Abstract

We present a comprehensive and self-contained discussion of the use of the transfer matrix to study propagation in one-dimensional lossless systems, including a variety of examples, such as superlattices, photonic crystals, and optical resonators. In all these cases, the transfer matrix has the same algebraic properties as the Lorentz group in a  $(2 + 1)$ -dimensional spacetime, as well as the group of unimodular real matrices underlying the structure of the  $abcd$  law, which explains many subtle details. We elaborate on the geometrical interpretation of the transfer-matrix action as a mapping on the unit disk and apply a simple trace criterion to classify the systems into three types with very different geometrical and physical properties. This approach is applied to some practical examples and, in particular, an alternative framework to deal with periodic (and quasiperiodic) systems is proposed.

**Keywords:** Transfer matrix, hyperbolic geometry, periodic systems

---

## Contents

<b>1</b>	<b>Introduction</b>	<b>2</b>
<b>2</b>	<b>Transfer matrix in quantum mechanics</b>	<b>3</b>
2.1	Basic concepts on transfer matrix . . . . .	3
2.2	Building the transfer matrix . . . . .	7
2.3	Hyperbolic Stokes parameters . . . . .	8
2.4	Lorentz transformation associated to a transfer matrix . . . . .	10
<b>3</b>	<b>Transfer matrix in other contexts</b>	<b>12</b>
3.1	Mechanical waves . . . . .	12
3.2	Electromagnetic waves . . . . .	12
3.3	Geometrical optics . . . . .	14
<b>4</b>	<b>The geometry of the transfer matrix</b>	<b>16</b>
4.1	Transfer function in the unit disc . . . . .	16
4.2	Transfer function in the half-plane . . . . .	20
4.3	Factoring the transfer matrix . . . . .	22
4.4	Geometrical reflections as building blocks . . . . .	23

<b>5</b>	<b>A closer look at the composition of transfer matrices</b>	<b>26</b>
5.1	Setting up the inverse system . . . . .	26
5.2	The Wigner angle . . . . .	28
5.3	Hyperbolic turns . . . . .	30
<b>6</b>	<b>Periodic systems</b>	<b>32</b>
6.1	Finite periodic structures . . . . .	32
6.2	Bandgaps in the unit disc . . . . .	34
6.3	Bandgaps in the half-plane . . . . .	36
6.4	Quasiperiodic sequences . . . . .	38
6.5	Hyperbolic tilings . . . . .	42
<b>7</b>	<b>Concluding remarks</b>	<b>44</b>

## 1. Introduction

Quantum mechanical scattering in one dimension describes many actual phenomena to a good approximation. The advantage of this theory is that it does not need special mathematical functions, while still retaining sufficient complexity to illustrate the pertinent physical concepts. It is therefore not surprising that there have been many articles dealing with various aspects of such scattering at various levels of detail, ranging from pedagogical issues (Eberly, 1965; James, 1970; Formánek, 1976; Kamal, 1984; van Dijk and Kiers, 1992; Nogami and Ross, 1996; Bartlette et al., 2000, 2001; Cattapan and Maglione, 2003; Sánchez-Soto et al., 2005; Boonserm and Visser, 2010b) to edge-cutting research (Peres, 1983; Jaworski and Wardlaw, 1989; Trzeciakowski and Gurioli, 1993; Sassoli-de-Bianchi, 1994; Rozman et al., 1994a; Nöckel and Stone, 1994; Sassoli-de-Bianchi and Ventra, 1995; Chebotarev and Tchepotareva, 1996; Kiers and van Dijk, 1996; Marinov and Segev, 1996; Kerimov and Sezgin, 1998; Visser, 1999; Miyazawa, 2000; Grossel et al., 2002; Boya, 2008; Xuereb et al., 2009; Boonserm and Visser, 2009, 2010a).

These papers emphasize notions such as partial-wave decomposition, Lippmann-Schwinger integral equations, transition operator, or parity-eigenstate representation, paralleling as much as possible their analogues in two and three dimensions. In other words, these approaches, like most of the standard textbooks on the subject (Goldberger and Watson, 1964; Newton, 1966; Cohen-Tannoudji et al., 1977; Galindo and Pascual, 1990), employ the  $S$  matrix [note some significant exceptions, such as, e.g. Mathews and Venkatesan (1978), Merzbacher (1997), Ballentine (1998), or Singh (1997)].

The elegance and power of the  $S$ -matrix formulation is beyond doubt. However, it is a “black-box” theory: the system under study is isolated and is tested through asymptotic states. This is well suited for experiments in elementary particle physics, but becomes inadequate as soon as one couples several systems. The most effective technique for studying such a coupling is the transfer matrix, in which the amplitudes of two fundamental solutions on either sides of a potential are connected by a matrix  $M$ .

The transfer matrix is a fruitful object widely used in the treatment of layered systems, like superlattices (Tsu and Esaki, 1973; Esaki, 1986; Ram-Mohan et al., 1988; Hauge and Stoveng, 1989; Vinter and Weisbuch, 1991; Weber, 1994; Sprung et al., 2003) or photonic crystals (Joannopoulos et al., 1995; Bendickson et al., 1996; Tsai et al., 1998). Optics, of course, is a field in which multilayers are important and the method is time honored (Brekovskikh, 1960; Lekner, 1987; Azzam and Bashara, 1987; Yeh, 1988).

An extensive and up-to-date review of the applications of the transfer matrix to many problems can be found in the two excellent monographs by García-Moliner and Velasco (1992) and Pérez-Álvarez and García-Moliner (2004). They are addressed to anyone who wants to enter the field and provide a really professional level of penetration into the basic issues.

A natural question thus arises: why yet another essay on the transfer matrix? The answer is simple: a quick look at the literature immediately reveals the different backgrounds and habits in which the transfer matrix is used and the very little “cross talk” between them. In fact, many scientists are usually not aware of the mathematical basis behind the standard toolkits they are using in their everyday research. The main goal of this review is precisely to fill this gap.

When one thinks in a unifying mathematical scenario, geometry immediately comes to mind. Although special relativity is the archetypal example of the interplay between physics and geometry, one cannot forget that geometrical ideas are essential in the development of modern physics (Schutz, 1997; Kauderer, 1994).

In recent years a number of geometrical concepts have been exploited to gain further insights into the behavior of scattering in one dimension (Yonete et al., 2002; Monzón et al., 2002; Barriuso et al., 2003a, 2004; Sprung et al., 2004; Martorell et al., 2004; Sánchez-Soto et al., 2005; Barriuso et al., 2009). The algebraic basis for these developments is the fact that the transfer matrix is an element of the group  $SU(1, 1)$ , which is locally isomorphic to the  $(2 + 1)$ -dimensional Lorentz group  $SO(2, 1)$ . This leads to a natural and complete identification between reflection and transmission coefficients and the parameters of the corresponding Lorentz transformation.

As soon as one realizes that  $SU(1, 1)$  is also the basic group of hyperbolic geometry (Coxeter, 1968), it is tempting to look for an enriching geometrical interpretation. In fact, we propose to look at the action of the transfer matrix as a bilinear (or Möbius) transformation on the unit disk, obtained by stereographic projection of the unit hyperboloid associated with  $SO(2, 1)$ .

Borrowing elementary techniques of hyperbolic geometry, we can classify and reinterpret all the relevant features of these matrices in a very elegant and concise way, largely independent of the model considered. We stress that this formulation does not offer any inherent advantage in terms of efficiency in solving practical problems; rather, we expect that it could supply a general and unifying setting to analyze the transfer matrix in many fields of physics, which, in our opinion, is more than a curiosity.

## 2. Transfer matrix in quantum mechanics

### 2.1. Basic concepts on transfer matrix

We consider the quantum scattering of a particle of mass  $m$  in one spatial dimension by a potential barrier  $V(x)$ . This is governed by the time-independent Schrödinger equation

$$\left[ -\frac{d^2}{dx^2} + U(x) \right] \Psi(x) = \varepsilon \Psi(x), \quad (1)$$

where

$$\varepsilon = \frac{2m}{\hbar^2} E, \quad U(x) = \frac{2m}{\hbar^2} V(x), \quad (2)$$

$E$  being the energy of the particle. We assume this potential to be real (i. e., a Hermitian operator) but otherwise arbitrary in a finite interval  $(a, b)$ . Outside this interval it is taken to be a constant that we define to be the zero of energy. Complex potentials can be used to model absorption, a situation which we shall not touch upon (Monzón et al., 2011).

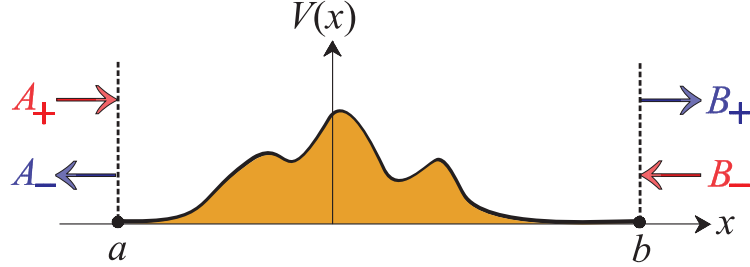


Figure 1: Illustration of the scattering from an arbitrary potential barrier, showing the input ( $A_+$  and  $B_-$ ) and output ( $A_-$  and  $B_+$ ) amplitudes.

The treatment can be also adapted, with minor modifications, to deal with potentials for which  $V_a \neq V_b$ , and also with the more subtle case of a position-dependent effective mass  $m(x)$ , which usually arise in superlattices (Leibler, 1975; Bastard, 1981; Pérez-Álvarez and Rodríguez-Coppola, 1988; Thomsen et al., 1989; Burt, 1992).

Since  $E > 0$ , the spectrum is continuous and we have two linearly independent solutions for a given value of  $E$  (Galindo and Pascual, 1990). Accordingly, the general solution of the time-independent Schrödinger equation can be expressed as a superposition of a right-mover  $e^{+ikx}$  and a left-mover  $e^{-ikx}$ :

$$\Psi(x) = \begin{cases} A_+ e^{+ik(x-a)} + A_- e^{-ik(x-a)} & x < a, \\ \Psi_{ab}(x) & a < x < b, \\ B_+ e^{+ik(x-b)} + B_- e^{-ik(x-b)} & x > b, \end{cases} \quad (3)$$

where  $k^2 = \varepsilon$  and the subscripts  $+$  and  $-$  indicate that the waves propagate to the right and to the left, respectively (see figure 1). The origins of the movers have been chosen to simplify the subsequent calculations.

To solve the problem in a closed form one must work out the Schrödinger equation in  $(a, b)$  to compute  $\Psi_{ab}(x)$  and invoke the appropriate boundary conditions, involving not only the continuity of  $\Psi(x)$  itself, but also of its derivative. In this way, one has two linear relations among the coefficients  $A_{\pm}$  and  $B_{\pm}$ , which can be solved for any amplitude pair in terms of the other two: the result can be expressed as a matrix equation, which translates the linearity of the problem. For our purposes, it is more advantageous to express a linear relation between the wave amplitudes on both sides of the scatterer, namely,

$$\begin{pmatrix} A_+ \\ A_- \end{pmatrix} = M_{ab} \begin{pmatrix} B_+ \\ B_- \end{pmatrix}, \quad (4)$$

$M_{ab}$  being the transfer matrix for the potential.

The reflection and transmission coefficients are the ratio of the amplitudes of the reflected and transmitted waves to the amplitude of the incoming wave, respectively. Denoting the amplitudes for waves propagating from the right as  $r_{ba}$  and  $t_{ba}$  and repeating the procedure, one easily finds that time-reversal invariance imposes

$$t_{ab} = t_{ba}, \quad r_{ba}/t_{ba} = -r_{ab}^*/t_{ab}^*, \quad (5)$$

while the conservation of the flux (??) gives

$$|r_{ab}|^2 + |t_{ab}|^2 = 1. \quad (6)$$

In conclusion, the form of the transfer matrix is

$$\mathbf{M}_{ab} = \begin{pmatrix} 1/t_{ab} & r_{ab}^*/t_{ab}^* \\ r_{ab}/t_{ab} & 1/t_{ab}^* \end{pmatrix}. \quad (7)$$

In the particular case of a symmetric potential [i.e.,  $V(x) = V(-x)$ ], it is clear that  $r_{ab} = r_{ba}$  and therefore the matrix element  $\beta$  is an imaginary number.

Thus far, we have related the amplitudes  $A_{\pm}$  to the  $B_{\pm}$ , as in equation (4). This choice is by no means essential and we could relate the amplitudes taken in the reverse order. The corresponding transfer matrix, represented by  $\mathbf{M}_{ba}$ , can be expressed as

$$\mathbf{M}_{ba} = \begin{pmatrix} 1/t_{ab} & -r_{ab}/t_{ab} \\ -r_{ab}^*/t_{ab}^* & 1/t_{ab}^* \end{pmatrix}, \quad (8)$$

where we have used (5).

We will now bring up the paradigmatic example when the potential  $V(x)$  reduces to a rectangular potential barrier of width  $L$  and height  $V_0$ . The calculations can be easily carried out, so we skip the details (Cohen-Tannoudji et al., 1977) and simply quote the results for  $r_{ab}$  and  $t_{ab}$  (with the choice of movers in figure 1)

$$\begin{aligned} r_{ab} &= \frac{(k^2 - \kappa^2) \sin(\kappa L)}{(k^2 + \kappa^2) \sin(\kappa L) + 2ik\kappa \cos(\kappa L)}, \\ t_{ab} &= \frac{2ik\kappa}{(k^2 + \kappa^2) \sin(\kappa L) + 2ik\kappa \cosh(\kappa L)}, \end{aligned} \quad (9)$$

with  $\kappa^2 = 2m(E - V_0)/\hbar^2$ . These coefficients correspond to  $E > V_0$ . When  $E < V_0$  the expressions are

$$\begin{aligned} r_{ab} &= \frac{(k^2 + \bar{\kappa}^2) \sinh(\bar{\kappa} L)}{(k^2 - \bar{\kappa}^2) \sinh(\bar{\kappa} L) + 2ik\bar{\kappa} \cosh(\bar{\kappa} L)}, \\ t_{ab} &= \frac{2ik\bar{\kappa}}{(k^2 - \bar{\kappa}^2) \sinh(\bar{\kappa} L) + 2ik\bar{\kappa} \cosh(\bar{\kappa} L)}, \end{aligned} \quad (10)$$

where now  $\bar{\kappa}^2 = 2m(V_0 - E)/\hbar^2$ . This can be obtained from the previous case with the formal substitution  $\bar{\kappa} \rightarrow i\kappa$ . Finally, when  $E = V_0$  a limiting procedure yields

$$r_{ab} = \frac{kL}{kL + 2i}, \quad t_{ab} = \frac{2i}{kL + 2i}. \quad (11)$$

A detailed discussion of the significance of these three situations can be found in Bohm (1989).

It is worth stressing that one could also relate outgoing amplitudes in terms of the incoming amplitudes (which are the magnitudes one can externally control). This is precisely the scattering matrix, which can be concisely written as

$$\begin{pmatrix} B_+ \\ A_- \end{pmatrix} = \mathbf{S}_{ab} \begin{pmatrix} A_+ \\ B_- \end{pmatrix}, \quad (12)$$

and  $S_{ab}$  reads

$$S_{ab} = \begin{pmatrix} t_{ab} & r_{ba} \\ r_{ab} & t_{ba} \end{pmatrix}. \quad (13)$$

Due to the properties (5) and (6),  $S_{ab}$  is unitary and with unit determinant, that is, an element of the group  $SU(2)$ .

Note carefully that the transfer matrix depends on the choice of basis vectors (Pérez-Álvarez et al., 2001; Pérez-Álvarez and García-Moliner, 2004) and special care must be paid when comparing results from different sources. For example, instead of specifying the amplitudes of the right and left-moving waves, we could also write a linear relation between the values of the wave function and its derivative at the points  $a$  and  $b$  (Sprung et al., 1993). prefer to employ the adimensional variables

$$\Psi(x) + \frac{1}{k}\Psi'(x), \quad \Psi(x) - \frac{1}{k}\Psi'(x). \quad (14)$$

This looks very much as passing from position-momentum to creation-annihilation operators (Baldentine, 1998). The amplitudes  $\mathcal{A}_\pm$  associated to these variables are related to  $A_\pm$  by

$$\begin{pmatrix} \mathcal{A}_+ \\ \mathcal{A}_- \end{pmatrix} = \mathcal{U} \begin{pmatrix} A_+ \\ A_- \end{pmatrix}, \quad (15)$$

with

$$\mathcal{U} = \frac{1}{\sqrt{2}} \begin{pmatrix} 1 & i \\ i & 1 \end{pmatrix}, \quad (16)$$

and analogously at the point  $b$ . The transfer matrix in this equivalent representation is

$$\mathcal{M}_{ab} = \mathcal{U} M_{ab} \mathcal{U}^\dagger = \begin{pmatrix} a & b \\ c & d \end{pmatrix}, \quad (17)$$

where  $\dagger$  stands for the Hermitian conjugate and

$$\begin{aligned} a &= \operatorname{Re} \alpha + \operatorname{Im} \beta, & b &= \operatorname{Im} \alpha + \operatorname{Re} \beta, \\ c &= -\operatorname{Im} \alpha + \operatorname{Re} \beta, & d &= \operatorname{Re} \alpha - \operatorname{Im} \beta, \end{aligned} \quad (18)$$

are real numbers. The role that the transformation  $\mathcal{U}$  will play in what follows justifies our choice in (14).

Since the determinant are preserved by matrix conjugation, we have that  $\det \mathcal{M}_{ab} = +1$ . In other words, the matrices  $\mathcal{M}_{ab}$  belong to the group  $SL(2, \mathbb{R})$  of unimodular  $2 \times 2$  matrices with real elements. The transformation by  $\mathcal{U}$  establishes in fact a one-to-one map between the group  $SL(2, \mathbb{R})$  of matrices  $\mathcal{M}_{ab}$  and the group  $SU(1, 1)$  of matrices  $M_{ab}$ , which allows for a direct translation of the properties from one to the other, as we will have occasion to check.

Irrespective of the representation used, transfer matrices are very convenient mathematical objects. Suppose we know how the wave functions “propagate” from point  $b$  to point  $a$ , with a transfer matrix we symbolically write as  $M_{ab}$ , and also from  $c$  to  $b$ , with  $M_{bc}$ . The crucial point is that the propagation from  $c$  to  $a$  is described by the product

$$M_{ac} = M_{ab} M_{bc}. \quad (19)$$

This property is rather helpful: we can connect simple scatterers to create an intricate potential landscape and determine its transfer matrix by simple multiplication (Jonsson and Eng, 1990; Kalotas and Lee, 1991; Walker and Gathright, 1994; Rozman et al., 1994a; Yuan et al., 2010). However, this important property does not seem to carry over into the scattering matrix in any simple way (Aktosun, 1992; Aktosun et al., 1996; Giust et al., 2009), because the incoming amplitudes for the overall system cannot be obtained in terms of the incoming amplitudes for every subsystem. While this is not a difficulty for a single scatterer (the typical situation arising in particle physics and for which the S-approach was specially tailored), it constitutes a drawback in applications where a number of cascaded systems are present.

## 2.2. Building the transfer matrix

The complete determination of the transfer matrix for an arbitrary potential  $V(x)$  amounts to solving the Schrödinger equation and, in consequence, it is not, in general, a simple exercise. Very accurate approximation schemes are available, among which we cite the WKB (Chebotarev, 1995, 1997), the variational (Bastard et al., 1983; Ahn and Chuang, 1986; Gould, 1995; Ando et al., 2003), the Monte-Carlo (Singh, 1986; Kalos and Whitlock, 2007), or the finite-element methods (Hayata et al., 1988; Nakamura et al., 1989; Ram-Mohan, 2002; Liu et al., 2004).

Here, we favor a method inspired by the long experience in dealing with layered systems (Kennett, 1983; Pérez-Álvarez et al., 1988; Rodríguez-Coppola et al., 1990; García-Moliner and Velasco, 1992; Pérez-Álvarez and García-Moliner, 2004). Roughly speaking, the idea is that one can consider  $V(x)$  as made of successive constant barriers, as schematized in figure 2 (Kalotas and Lee, 1991; Rozman et al., 1994b; Grossel et al., 1994; Cao et al., 2001; Rakityansky, 2004; He et al., 2005; Monsoriu et al., 2005; Su et al., 2008; Hutem and Sricheewin, 2008; Wen et al., 2010). The  $j$ th barrier, of height  $V_j$  and width  $d_j$ , is situated between the points  $x_{j-1}$  and  $x_j$  (we take  $x_0 = a$  and  $x_{N+1} = b$ ). In this way, we express  $M_{ab}$  as a product of matrices that characterize the effects of the individual discontinuities and propagations of the entire discretized structure, taken in the proper order, as follows (Yeh, 1988):

$$M_{ab} = l_{01} P_1 l_{12} P_2 l_{23} \dots l_{(j-1)j} P_j l_{j(j+1)} \dots l_{(N-1)N} P_N l_{N(N+1)}. \quad (20)$$

When the number of barriers is large enough, the method should provide satisfactory results for any potential (Jirauschek, 2009). Here  $l_{ij}$  accounts for the discontinuity at the interface between  $V_i$  and  $V_j$ , and has the form (Landau and Lifshitz, 2001)

$$l_{ij} = \frac{1}{t_{ij}} \begin{pmatrix} 1 & r_{ij} \\ r_{ij} & 1 \end{pmatrix}, \quad (21)$$

where  $r_{ij}$  and  $t_{ij}$  are the reflection and transmission coefficients at the interface  $ij$  and are given by

$$r_{ij} = \frac{\kappa_i - \kappa_j}{\kappa_i + \kappa_j}, \quad t_{ij} = \frac{2\kappa_i}{\kappa_i + \kappa_j}. \quad (22)$$

The wave number is  $\kappa_j^2 = 2m(E - V_j)/\hbar^2$  and, for simplicity, we have assumed  $E > V_j$ . They verify

$$\det l_{ij} = \frac{\kappa_j}{\kappa_i}, \quad (23)$$

and the outstanding composition law

$$l_{ij} l_{j(j+1)} = l_{i(j+1)}. \quad (24)$$

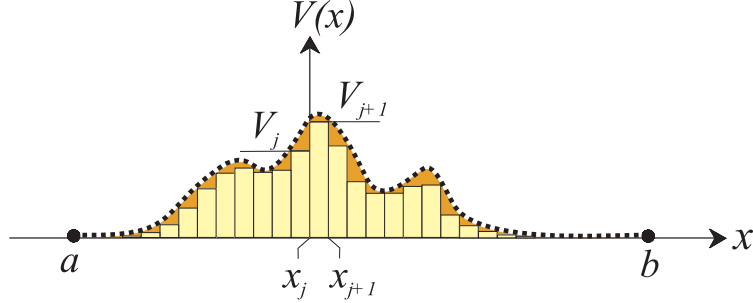


Figure 2: Decomposition of the potential  $V(x)$  in elementary rectangular barriers.

The matrix  $P_j$  describes the effect of propagation through the barrier  $j$  alone, and reads

$$P_j = \begin{pmatrix} \exp(i\delta_j) & 0 \\ 0 & \exp(-i\delta_j) \end{pmatrix}, \quad (25)$$

where the phase shift is  $\delta_j = \kappa_j d_j$ . Now, we have

$$\det P_j = 1. \quad (26)$$

By taking the determinant in equation (20) and using (23) and (26) we get a simple but relevant result:

$$\det M_{ab} = \frac{\kappa_{N+1}}{\kappa_0} = \frac{t_{ba}}{t_{ab}}. \quad (27)$$

Therefore, when  $V_a$  and  $V_b$  are the same (as we have assumed until now), the determinant of  $M_{ab}$  is +1. When these potentials are different, this result also holds by renormalizing conveniently the amplitudes (Monzón and Sánchez-Soto, 1999).

If we denote

$$M_j = I_{0j} P_j I_{j0}, \quad (28)$$

which corresponds to the  $j$ th barrier sandwiched between two identical constant potentials (that for simplicity we take as 0), we can also rewrite equation (20) as

$$M_{ab} = \prod_{j=1}^N M_j. \quad (29)$$

Sometimes, it is more convenient to work with unimodular matrices in  $SL(2, \mathbb{R})$ . The counterparts of interface and propagation can be obtained by conjugating (21) and (25) with  $\mathcal{U}$ ; the final result is

$$\mathcal{I}_{ij} = \frac{1}{t_{ij}} \begin{pmatrix} 1 & r_{ij} \\ r_{ij} & 1 \end{pmatrix}, \quad \mathcal{P}_j = \begin{pmatrix} \cos \delta_j & \sin \delta_j \\ -\sin \delta_j & \cos \delta_j \end{pmatrix}. \quad (30)$$

### 2.3. Hyperbolic Stokes parameters

To move ahead let us construct the matrices

$$J = \begin{pmatrix} X_+ \\ X_- \end{pmatrix} \otimes \begin{pmatrix} X_+^* & X_-^* \end{pmatrix} = \begin{pmatrix} |X_+|^2 & X_+ X_-^* \\ X_+^* X_- & |X_-|^2 \end{pmatrix}, \quad (31)$$



where  $X = A$  or  $B$  are the amplitudes that determine the behavior at the points  $a$  and  $b$ , respectively. They are quite reminiscent of the coherence matrix in optics or the density matrix in quantum mechanics (Mandel and Wolf, 1995). Observe that  $J$  is Hermitian and  $\det J = 0$ . In addition, one can readily verify that

$$J_a = M_{ab} J_b M_{ab}^\dagger, \quad (32)$$

so they transform under  $M_{ab}$  by congruence.

Let now  $\sigma_\mu$  (the Greek indices run from 0 to 3) be the set of four Hermitian matrices  $\sigma_0 = \mathbb{1}$  (the identity) and  $(\sigma_1, \sigma_2, \sigma_3)$  (the standard Pauli matrices). They constitute a natural basis of the vector space of  $2 \times 2$  complex matrices, so the coordinates  $s^\mu$  with respect to that basis are

$$s^\mu = \frac{1}{2} \text{Tr}(J \sigma_\mu), \quad (33)$$

so that

$$\begin{aligned} s^0 &= \frac{1}{2}(|X_+|^2 + |X_-|^2), \\ s^1 &= \text{Re}(X_+^* X_-), \\ s^2 &= \text{Im}(X_+^* X_-), \\ s^3 &= \frac{1}{2}(|X_+|^2 - |X_-|^2). \end{aligned} \quad (34)$$

The congruence (32) induces in this manner a transformation on the variables  $s^\mu$  of the form

$$s_a^\mu = \Lambda^\mu_\nu s_b^\nu, \quad (35)$$

where  $\Lambda^\mu_\nu$  can be found to be

$$\Lambda^\mu_\nu(M_{ab}) = \frac{1}{2} \text{Tr}(\sigma_\mu M_{ab} \sigma_\nu M_{ab}^\dagger), \quad (36)$$

and it turns out to be a Lorentz transformation. This equation can be solved to obtain  $M_{ab}$  from  $\Lambda$ . The matrices  $M_{ab}$  and  $-M_{ab}$  generate the same  $\Lambda$ , so this homomorphism is two-to-one (Barut, 1980).

The variables  $s^\mu$  are coordinates in a Minkovskian space. Since  $\det J = 0$ , the value of the interval (in both points  $a$  and  $b$ ) is

$$(s^0)^2 - (s^1)^2 - (s^2)^2 - (s^3)^2 = 0, \quad (37)$$

so it is lightlike. Moreover, the conservation of the probability current expressed in equation (??) means that the coordinate  $s^3$ , defined in (34), remains invariant and (37) reduces to

$$(s^0)^2 - (s^1)^2 - (s^2)^2 = (s^3)^2 = \text{constant}, \quad (38)$$

that is, a two-sheeted hyperboloid of radius  $s^3$ , which without loss of generality will be taken henceforth as unity (see figure 3). All this shows that the group  $SU(1,1)$  of transfer matrices is locally isomorphic to the  $(2+1)$ -dimensional Lorentz group  $SO(2,1)$ . In fact, in more technical terms, the matrices  $M_{ab}$  form a two-dimensional spinor representation of the restricted Lorentz group  $SO(2,1)$ :  $\Lambda_1 \Lambda_2 \longleftrightarrow M(\Lambda_1) M(\Lambda_2) = \pm M(\Lambda_1 \Lambda_2)$ .

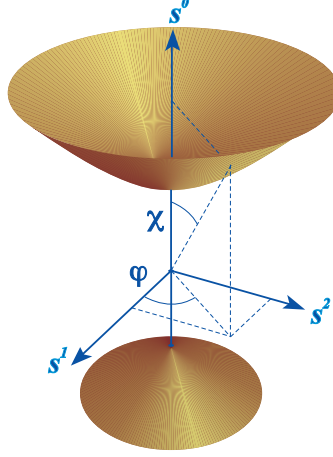


Figure 3: Pseudospherical coordinates of the unit two-sheeted hyperboloid associated with a transfer matrix  $M_{ab}$ .

Let us now rewrite the complex amplitudes  $X_{\pm}$  in polar form

$$X_{\pm} = |X_{\pm}| \exp(i\varphi_{\pm}). \quad (39)$$

Denoting  $\varphi = \varphi_+ - \varphi_-$  and introducing the angle  $\chi$  in pseudospherical coordinates (shown in figure 3), we have

$$\begin{aligned} s^0 &= \cosh \chi, \\ s^1 &= \sinh \chi \cos \varphi, \\ s^2 &= \sinh \chi \sin \varphi. \end{aligned} \quad (40)$$

This parametrization is very evocative of the standard one for the Stokes parameters in the unit Poincaré sphere (Born and Wolf, 1999), except for the fact that now the angle  $\chi$  appears as the argument of hyperbolic functions. We refer to these parameters as hyperbolic Stokes parameters. One can interpret the rotations  $\varphi$  and the hyperbolic rotations  $\chi$  much in the same way as it is done for the Poincaré sphere (Giust and Vigoureux, 2002): a rotation of angle  $\varphi$  about the axis  $s^0$  corresponds to a dephasing between left- and right-traveling waves without changing their relative amplitudes; as it happens, for example, in the propagation inside a barrier. On the contrary, a hyperbolic rotation of angle  $\chi$  corresponds to a change in amplitude between left- and right-traveling waves, as it occurs at the discontinuity between two barriers.

#### 2.4. Lorentz transformation associated to a transfer matrix

To better appreciate the physical meaning of the Lorentz transformation induced by a transfer matrix, we recall that a Lorentz transformation  $\Lambda$  can be always decomposed into a product of a spatial rotation  $R$  and a boost  $L$  along an arbitrary direction (Moretti, 2006)

$$\Lambda = L R. \quad (41)$$

The analogous factorization for a transfer matrix is the polar decomposition, which ensures that any matrix  $M \in \text{SU}(1,1)$  (to simplify the notation, we drop the subscript  $ab$  in the rest of this

section) can be expressed in a unique way as

$$M = HU, \quad (42)$$

where  $H$  is positive definite Hermitian (“modulus”) and  $U$  is unitary (“argument”). Under the homomorphism discussed previously,  $H$  generates a boost and  $U$  a rotation, in agreement with equation (41).

To find their explicit form we note that polar decomposition for the matrix  $M$  in equation (7) reads

$$M = HU = \frac{1}{|t|} \begin{pmatrix} 1 & r^* \\ r & 1 \end{pmatrix} \begin{pmatrix} \exp(-i\tau) & 0 \\ 0 & \exp(i\tau) \end{pmatrix}, \quad (43)$$

where we have expressed the reflection and transmission coefficients in the form

$$r = |r| \exp(i\rho), \quad t = |t| \exp(i\tau). \quad (44)$$

Using (36), the unitary component  $U$  generates the rotation [in  $(2+1)$  dimensions]

$$R(U) = \begin{pmatrix} 1 & 0 & 0 \\ 0 & \cos(2\tau) & -\sin(2\tau) \\ 0 & \sin(2\tau) & \cos(2\tau) \end{pmatrix}, \quad (45)$$

that is, a spatial rotation in the plane 1-2 of angle twice the phase of the transmission coefficient.

The Hermitian component  $H$  generates the boost

$$L(H) = \begin{pmatrix} \gamma & -\gamma v \cos \rho & -\gamma v \sin \rho \\ -\gamma v \cos \rho & 1 + (\gamma - 1) \cos^2 \rho & (\gamma - 1) \cos \rho \sin \rho \\ -\gamma v \sin \rho & (\gamma - 1) \cos \rho \sin \rho & 1 + (\gamma - 1) \sin^2 \rho \end{pmatrix}. \quad (46)$$

The modulus of the velocity  $v$  (we take  $c = 1$  everywhere) and the relativistic factor  $\gamma = 1/\sqrt{1-v^2}$  of this boost are

$$v = \frac{2|r|}{1+|r|^2}, \quad \gamma = \frac{1+|r|^2}{1-|r|^2}. \quad (47)$$

The matrix  $L(H)$  is then a boost to a reference frame moving with a constant velocity  $v$  in the plane 1–2, in a direction forming a counterclockwise angle  $\rho$  with the axis 1.

If, as it is usual, we introduce the rapidity  $\zeta$  from (Jackson, 1975)

$$v = \tanh \zeta, \quad (48)$$

we have the following appealing identification of the reflection and transmission coefficients with the parameters of the Lorentz transformation:

$$r = \tanh(\zeta/2) \exp(i\rho), \quad t = \operatorname{sech}(\zeta/2) \exp(i\tau). \quad (49)$$

Therefore,  $|r| = \tanh(\zeta/2)$ , behaves as a velocity, while  $|t|$  behaves as  $1/\gamma$ .

The convenient properties of the hyperbolic tangent have been exploited in dealing with layered systems (Khashan, 1979; Corzine et al., 1991), and explain why the reflection coefficients are examined in greater detail than the transmission ones.

### 3. Transfer matrix in other contexts

One-dimensional continuous models provide a detailed account of the behavior of a variety of systems (Lieb and Matthis, 1966; Albeverio et al., 2004). The nature of the actual particles, or states, or elementary excitations, as they may be variously called, is irrelevant for many purposes: there is always two input and two output channels related by a  $2 \times 2$  transfer matrix. In fact, this matrix can be viewed as a compact way of setting out the integration of the differential equations involved in the model with the pertinent boundary conditions; this is what makes the method so effective.

From this perspective, one can construct a general theory of the transfer matrix for second-order differential equations (Khorasani and Adibi, 2003; Khorasani and Mehrany, 2003). However, we prefer to explore some selected examples (Pérez-Álvarez and García-Moliner, 2004); this restricted choice reflects the authors personal bias, but it is illustrative enough to grasp what the method is about.

#### 3.1. Mechanical waves

Transverse waves on weighted strings, longitudinal waves on loaded rods, acoustic waves in corrugated tubes, and water waves crossing sandbars, among other examples (Griffiths and Steinke, 2001), are governed by the classical wave equation

$$\frac{\partial^2 \psi}{\partial t^2} = v^2 \frac{\partial^2 \psi}{\partial x^2}. \quad (50)$$

Here  $\psi(x, t)$  is the amplitude of the considered phenomena (in the above-mentioned examples  $\psi(x, t)$  stands for the transverse displacement of the string, the displacement of a point whose equilibrium position is  $x$ , the pressure above ambient, or the height of the surface above its equilibrium level, respectively), and  $v(x)$  is the local propagation speed of the perturbation. We continue to use complex notation, with the understanding that the physical wave is the real part. For a monochromatic perturbation of angular frequency  $\omega$  [ $\psi(x, t) = \Psi(x)e^{-i\omega t}$ ] equation (50) reduces to

$$\left[ \frac{d^2}{dx^2} + k^2(x) \right] \Psi(x) = 0, \quad (51)$$

and the local wave number is

$$k(x) = \frac{\omega}{v(x)}. \quad (52)$$

The expansion in left- and right-movers in section 2 can be transplanted here without modifications. In addition, as we did in 2.2, we can build the transfer matrix by assuming that the material parameters of the medium are piecewise constant and vary in a stepwise manner, so each constituent slab is a homogeneous material by itself. The mismatched impedances generate the reflected and transmitted waves (Crawford, 1968), while the application of the proper boundary conditions at the discontinuity points (which depend on the particular model under consideration) provide the corresponding amplitude coefficients.

#### 3.2. Electromagnetic waves

We next consider the propagation of plane electromagnetic waves in a (nonmagnetic) stratified medium, whose optical properties are contained in the dielectric function  $\epsilon(x) = n^2(x)$  [ $n(x)$

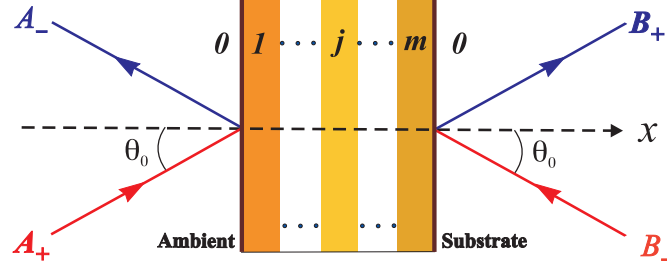


Figure 4: Amplitudes of the input [ $A_+$  and  $B_-$ ] and output [ $A_-$  and  $B_+$ ] fields in a multilayer sandwiched between two semi-infinite ambient and substrate identical media. The angle of refraction in the  $j$ th medium is denoted  $\theta_j$ .

is the local value of the refractive index]. For a monochromatic component of frequency  $\omega$  we write the field components as (Monsivais et al., 1995)

$$\mathbf{E}(\mathbf{r}, t) = \mathcal{E}(x) \exp[-i(\omega t - \mathbf{K} \cdot \mathbf{r})], \quad \mathbf{B}(\mathbf{r}, t) = \mathcal{B}(x) \exp[-i(\omega t - \mathbf{K} \cdot \mathbf{r})], \quad (53)$$

where  $\mathbf{K}$  is the component of the wave vector in the plane perpendicular to the  $x$  axis. By eliminating, e.g., the magnetic field  $\mathbf{B}$  from Maxwell equations, it turns out that (Born and Wolf, 1999)

$$\left[ \frac{d^2}{dx^2} + k^2(x) \right] \mathcal{E}(x) = 0, \quad (54)$$

and  $k(x)$  is the local value of the normal component of the wave vector

$$k(x) = \sqrt{\epsilon(x) \frac{\omega^2}{c^2} - K^2}. \quad (55)$$

A completely analogous equation can be written for the magnetic field by eliminating  $\mathbf{E}$ .

Apparently, equation (54) is identical to (51), and the theory can be immediately extended here, expressing the solution as a superposition of a left- and right-mover fields. But this requires some extra care because the amplitude in (54) is a vector.

For linear isotropic media, any plane wave can be written as a superposition of an  $s$  (or TE) wave and a  $p$  (or TM) wave. The  $s$  wave has its electric vector perpendicular to the plane of incidence, and the  $p$  wave has its electric vector in the plane of incidence (and its magnetic vector perpendicular to the plane of incidence; hence its designation as a TM, or transverse magnetic, wave). If we further take the plane of incidence to be the  $(x, z)$  plane, the vectors are (Azzam and Bashara, 1987; Lekner, 1987; Yeh, 1988)

$$\mathcal{E} = \begin{pmatrix} 0 \\ \mathcal{E}_y \\ 0 \end{pmatrix} \quad (s \text{ polarization}) \quad \mathcal{B} = \begin{pmatrix} 0 \\ \mathcal{B}_y \\ 0 \end{pmatrix} \quad (p \text{ polarization}). \quad (56)$$

This has to be taken into account when matching the boundary conditions between two media. For these two basic polarizations the problem reduces to a scalar one, and the transfer matrix can be applied as before.

If the medium extends from  $x = a$  to  $x = b$ , bounded by the same homogeneous media (ambient and substrate) of index  $n_0$ , the formal solution can be written in full analogy with equation (3) and one can use a transfer matrix that relates the field amplitudes  $A_{\pm}$  and  $B_{\pm}$ .

Again, one can take the medium as consisting of a stack of  $1, 2, \dots, j, \dots, m$  plane-parallel layers, as sketched in figure 4. We denote by  $n_j$ ,  $d_j$ , and  $\theta_j$ , respectively, the refractive index, the thickness, and the angle of refraction of the  $j$ th medium, which can be obtained by a repeated application of Snell's law (which is a consequence of the conservation of the modulus of  $\mathbf{K}$ )

$$n_0 \sin \theta_0 = \dots n_j \sin \theta_j = \dots = n_m \sin \theta_m. \quad (57)$$

The transfer matrix is given by the ordered product in equation (20) and the interface matrix has the same expression as in equation (21), but with

$$\begin{aligned} r_{ij}^p &= \frac{n_j \cos \theta_i - n_i \cos \theta_j}{n_j \cos \theta_i + n_i \cos \theta_j}, & t_{ij}^p &= \frac{2n_i \cos \theta_i}{n_j \cos \theta_i + n_i \cos \theta_j}, \\ r_{ij}^s &= \frac{n_i \cos \theta_i - n_j \cos \theta_j}{n_i \cos \theta_i + n_j \cos \theta_j}, & t_{ij}^s &= \frac{2n_i \cos \theta_i}{n_i \cos \theta_i + n_j \cos \theta_j}, \end{aligned} \quad (58)$$

for each one of the basic polarizations. The propagation matrix is also as in (25), but now the phase shift is

$$\delta_j = \frac{2\pi}{\lambda} n_j d_j \cos \theta_j, \quad (59)$$

$\lambda$  being the wavelength in vacuum. All this gives the formalism developed by Hayfield and White in terms of movers (Azzam and Bashara, 1987).

It is also possible to develop an equivalent formalism by employing the amplitudes in equation (15), which, roughly speaking, are the electric field and its derivative at each point. This is the idea behind the pioneering work of Abelès (1948).

### 3.3. Geometrical optics

Finally, we look at the paraxial propagation of light through axially symmetric systems, containing no tilted or misaligned elements (Wolf, 2004). We take a Cartesian coordinate system whose  $x$  axis is along the axis of the optical system (see figure 5) and represent a ray at a plane  $x$  by the transverse position vector  $q(x)$  (which can be chosen in the meridional plane) and by the momentum  $p(x) = n\theta(x)$ , which in the paraxial limit is  $p(x) = ndq(x)/dx$ , where  $n$  is the refractive index of the medium. These are canonical coordinates and satisfy all the mathematical requirements for a consistent description (Guillemin and Sternberg, 1984).

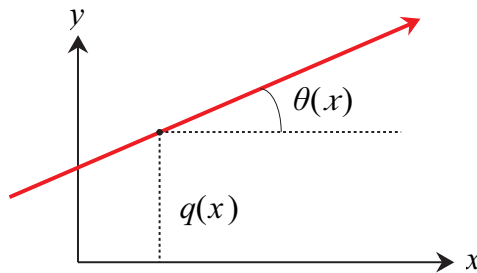


Figure 5: Notation for the ray vector. The optical axis is  $x$ ,  $q(x)$  is the transverse position at a point  $x$  reached by a ray and  $\theta$  is the ray inclination at that point.

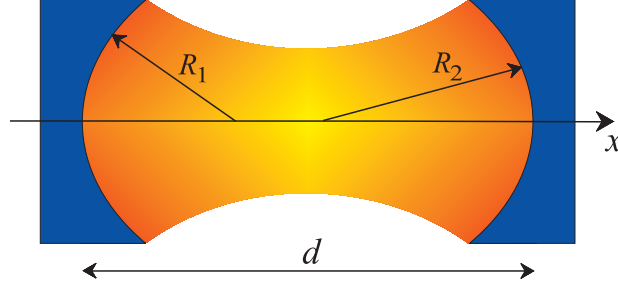


Figure 6: Optical cavity consisting of two spherical mirrors of radii  $R_1$  and  $R_2$  separated a distance  $d$ .

In homogeneous media, to fully specify the ray behavior three basic matrices are needed, namely

$$\begin{pmatrix} 1 & d/n \\ 0 & 1 \end{pmatrix}, \quad \begin{pmatrix} 1 & 0 \\ (n' - n)/R & 1 \end{pmatrix}, \quad \begin{pmatrix} 1 & 0 \\ -2n/R & 1 \end{pmatrix}. \quad (60)$$

The first one gives the propagation through a distance  $d$ , the second gives the changes in the ray parameters for a refraction in a dioptr of radius  $R$  separating two homogeneous media of refractive indices  $n$  and  $n'$ , and the third one is the reflection in a mirror of radius  $R$ .

Let us apply these matrices to the illustrative example of an optical cavity consisting of two spherical mirrors of radii  $R_1$  and  $R_2$ , separated a distance  $d$ , which will be examined in more detail in Section 6.3 (see figure 6). The ray-transfer matrix corresponding to a round trip can be routinely computed using (60) (Gerrard and Burch, 1975):

$$\mathcal{M} = \begin{pmatrix} 2g_1g_2 - g_1 + g_2 - 1 & \frac{d}{2}(2g_1g_2 + g_1 + g_2) \\ \frac{2}{d}(2g_1g_2 - g_1 - g_2) & 2g_1g_2 + g_1 - g_2 - 1 \end{pmatrix}, \quad (61)$$

where we have introduced the parameters ( $i = 1, 2$ )

$$g_i = 1 - \frac{d}{R_i}. \quad (62)$$

In the same vein, a general first-order system can be built as a cascaded application of these three basic elements and the ray parameters change according to the simple transformation (Simon and Wolf, 2000; Wolf, 2004; Bařkal et al., 2004)

$$\begin{pmatrix} q_a \\ p_a \end{pmatrix} = \mathcal{M}_{ab} \begin{pmatrix} q_b \\ p_b \end{pmatrix}, \quad (63)$$

and  $\mathcal{M}_{ab}$  is the ray-transfer matrix

$$\mathcal{M}_{ab} = \begin{pmatrix} a & b \\ c & d \end{pmatrix}. \quad (64)$$

Since the three basic matrices in (60) have unit determinant, this means that  $\det \mathcal{M} = +1$ , so that they belong to the group  $SL(2, \mathbb{R})$  of real unimodular  $2 \times 2$  matrices. This is the essence of the celebrated *abcd* law in geometrical optics.

## 4. The geometry of the transfer matrix

### 4.1. Transfer function in the unit disc

Let us go back to the unit two-sheeted hyperboloid (38) that is the phase space for our problem. If one uses stereographic projection taking the south pole  $S = (-1, 0, 0)$  as projection center (see figure 7), the projection of the point  $(s^0, s^1, s^2)$  becomes in the complex plane

$$z = \frac{s^1 + is^2}{1 + s^0} = \frac{X_-}{X_+}, \quad (65)$$

for  $X = A$  or  $B$ . This confirms that what matters here are the transformation properties of amplitude quotients rather than the amplitudes themselves. In terms of the pseudospherical coordinates (40), this point can be written as

$$z = \frac{\sinh \chi}{1 + \cosh \chi} \exp(i\varphi) = \tanh(\chi/2) \exp(i\varphi), \quad (66)$$

which allows to interpret  $\chi$  as a rapidity and  $\varphi$  as a phase shift. The upper sheet of the unit hyperboloid is projected into the unit disc, we shall denote  $\mathbb{D}$ , the lower sheet into the external region, while the infinity goes to the boundary of the unit disc. We mention in passing that stereographic projection is conformal, meaning that it preserves the angles at which curves cross each other on the two-sheeted hyperboloid.

Through stereographic projection, the standard Minkowski distance in the unit hyperboloid becomes in  $\mathbb{D}$  (Anderson, 1999)

$$ds^2 = \frac{dz dz^*}{(1 - |z|^2)^2}. \quad (67)$$

The geodesics in the hyperboloid are intersections with the hyperboloid of planes passing through the origin. Consequently, hyperbolic lines are obtained from these by stereographic projection and they correspond to circle arcs that orthogonally cut the boundary of the unit disk (diameters are a particular instance of these geodesics), as equation (67) confirms after some calculations (Mischenko and Fomenko, 1988).

It seems natural to consider the complex variables in equation (65) for both points  $a$  and  $b$ . The basic linear relation expressed in equation (4) settles a transformation on the complex plane  $\mathbb{C}$ , mapping the point  $z_b$  into the point  $z_a$  according to

$$z_a = \Phi[M_{ab}, z_b] = \frac{\alpha^* z_b + \beta^*}{\beta z_b + \alpha}, \quad (68)$$

which is a bilinear or Möbius transformation. The action of the transfer matrix appears then as a function  $z_a = f(z_b)$  that can be appropriately called the transfer function (Yonte et al., 2002). One can check that the unit disk  $\mathbb{D}$ , the external region and the boundary remain also invariant under this action.

We shall need the concept of hyperbolic distance in the unit disc. To this end, it is customary to define the cross ratio of four distinct points  $z_A, z_B, z_C$ , and  $z_D$  as the number

$$(z_A, z_B | z_C, z_D) = \frac{(z_A - z_C)(z_B - z_D)}{(z_A - z_D)(z_B - z_C)}, \quad (69)$$

which is real only when the four points lie on a circle or a straight line. In fact, bilinear transformations preserve this cross ratio (Pedoe, 1970).



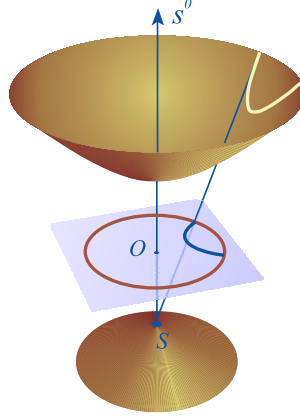


Figure 7: Outline of the unit hyperboloid and a geodesic on it. We also show how a hyperbolic line is obtained in the unit disk by stereographic projection, taking the south pole as projection center.

Let now  $z$  and  $z'$  be two points that are joined by the hyperbolic line whose endpoints on the unit circle are  $e$  and  $e'$ . The hyperbolic distance between  $z$  and  $z'$  is

$$d_H(z, z') = \frac{1}{2} |\ln(e, e' | z, z')|. \quad (70)$$

The fundamental point for us is that bilinear transformations are isometries; i.e., they preserve this distance.

The visual import of the disk with this metric is that a pair of points with a given distance between will appear to be closer and closer as their location approaches the boundary circle. Or, equivalently, a pair of points near the unit circle are actually farther apart (via the metric) than a pair near the center of the disc, which appear to be the same distance apart.

An important tool for the classification of the transfer-matrix action are the fixed points, which correspond to the wave functions such that  $z_a = z_b$  in equation (68). If we denote them by  $z_f$  we have that

$$z_f = \Phi[M_{ab}, z_f], \quad (71)$$

whose solutions are

$$z_{f\pm} = \frac{1}{2\beta} \left\{ -2i \operatorname{Im}(\alpha) \pm \sqrt{[\operatorname{Tr}(M_{ab})]^2 - 4} \right\}. \quad (72)$$

When  $|\operatorname{Tr}(M_{ab})| < 2$  the action is said elliptic and it has only one fixed point inside  $\mathbb{D}$ , while the other lies outside. Since in the Euclidean geometry a rotation is characterized for having only one invariant point, this action can be appropriately called a hyperbolic rotation.

When  $|\operatorname{Tr}(M_{ab})| > 2$  the action is hyperbolic and it has two fixed points both on the boundary of  $\mathbb{D}$ . The hyperbolic line joining these two fixed points remains invariant and thus, by analogy with the Euclidean case, this action will be named a hyperbolic translation.

Finally, when  $|\operatorname{Tr}(M_{ab})| = 2$  the action is parabolic and it has only one (double) fixed point on the boundary of  $\mathbb{D}$ . This action has no Euclidean analogy and will be called a parallel displacement for reasons that will become clear soon.

It is worth mentioning that for the example of the rectangular barrier discussed in equations (9)-(11), the associated actions are elliptic, hyperbolic, or parabolic according to whether  $E$  is greater than, less than, or equal to  $V_0$ , respectively.

To proceed further, let us note that by taking the conjugate of  $M_{ab}$  with any matrix  $C \in \text{SU}(1, 1)$ ; i.e.,

$$\hat{M}_{ab} = C M_{ab} C^{-1}, \quad (73)$$

we get another matrix of the same type, forasmuch as  $\text{Tr}(\hat{M}_{ab}) = \text{Tr}(M_{ab})$ . Conversely, if two transfer matrices have the same trace, one can always find a matrix  $C$  satisfying equation (73). The fixed points of  $\hat{M}_{ab}$  are the image by  $C$  of the fixed points of  $M_{ab}$ . In fact, if we write the matrix  $C$  as

$$C = \begin{pmatrix} c_1 & c_2 \\ c_2^* & c_1^* \end{pmatrix}, \quad (74)$$

the matrix elements of  $\hat{M}_{ab}$  (marked by carets) and those of  $M_{ab}$  are related by

$$\begin{aligned} \hat{\alpha} &= \alpha |c_1|^2 - \alpha^* |c_2|^2 - 2i \text{Im}(\beta c_1 c_2^*), \\ \hat{\beta} &= \beta c_1^2 - \beta^* c_2^2 - 2i c_1 c_2 \text{Im}(\alpha). \end{aligned} \quad (75)$$

In consequence, given any transfer matrix  $M_{ab}$  one can always reduce it to a  $\hat{M}_{ab}$  with one of the following canonical forms

$$\begin{aligned} \hat{K}(\phi) &= \begin{pmatrix} \exp(i\phi/2) & 0 \\ 0 & \exp(-i\phi/2) \end{pmatrix}, \\ \hat{A}(\xi) &= \begin{pmatrix} \cosh(\xi/2) & i \sinh(\xi/2) \\ -i \sinh(\xi/2) & \cosh(\xi/2) \end{pmatrix}, \\ \hat{N}(\nu) &= \begin{pmatrix} 1 - i\nu/2 & \nu/2 \\ \nu/2 & 1 + i\nu/2 \end{pmatrix}, \end{aligned} \quad (76)$$

where  $0 \leq \phi \leq 4\pi$  and  $\xi, \nu \in \mathbb{R}$ . They have as fixed points the origin (elliptic),  $+i$  and  $-i$  (hyperbolic) and  $+i$  (parabolic). All these  $\text{SU}(1, 1)$  matrices leave invariant  $|X_+|^2 - |X_-|^2$  at each side of the potential, in agreement with equation (??). In addition,  $\hat{K}(\phi)$  preserves the product  $X_+ X_-$ ,  $\hat{A}(\xi)$  preserves the quadratic form  $X_+^2 + X_-^2$ , and  $\hat{N}(\nu)$  preserves the sum  $X_+ + i X_-$  (Yonke et al., 2002).

The matrix  $\hat{K}(\phi)$  represents the free propagation in a constant potential barrier with a dephasing of  $\phi/2$ . Obviously, this reduces to a mere shift of the origin of phases. The second matrix  $\hat{A}(\xi)$  represents a symmetric system with reflection and transmission phase shifts of  $\tau_{\hat{A}} = 0$  and  $\rho_{\hat{A}} = \pm\pi/2$ , and a transmission coefficient  $t_{\hat{A}} = \text{sech}(\xi/2)$ . Finally, the third matrix,  $\hat{N}(\nu)$ , represents a system having  $t_{\hat{N}} = \cos(\tau_{\hat{N}}) \exp(i\tau_{\hat{N}})$  and  $r_{\hat{N}} = \sin(\tau_{\hat{N}}) \exp(i\tau_{\hat{N}})$ , with  $\tan(\tau_{\hat{N}}) = \nu/2$ . There are many ways to implement these elementary actions depending on the physical system under consideration (Simon and Mukunda, 1998).

The explicit construction of the family of matrices  $C$  is easy: it suffices to impose that  $C$  transforms the fixed points of  $M_{ab}$  into the ones of  $\hat{K}(\phi)$ ,  $\hat{A}(\xi)$ , or  $\hat{N}(\nu)$ . By way of example, let us examine the case when  $M_{ab}$  is elliptic and its fixed point inside the unit disk is  $z_f$ . One should have

$$\Phi[CM_{ab}C^{-1}, 0] = \Phi[CM_{ab}, z_f] = \Phi[C, z_f] = 0. \quad (77)$$

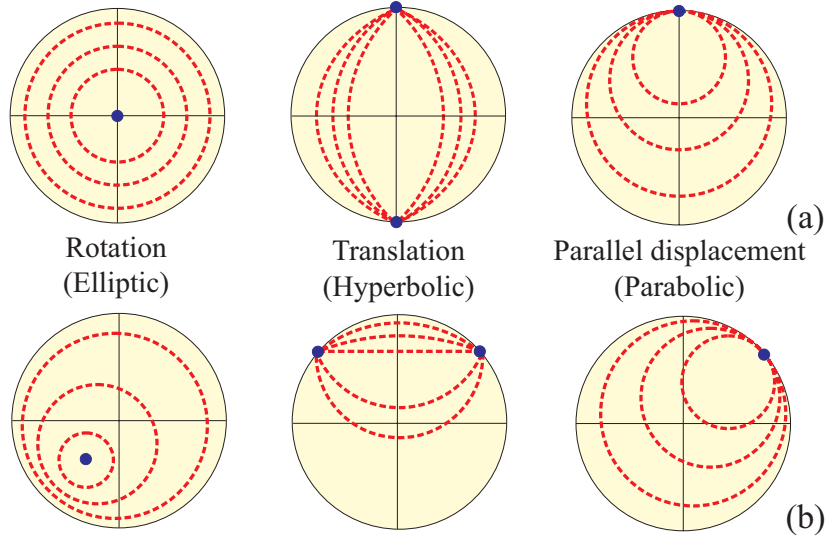


Figure 8: Plot of orbits in the unit disk for: (a) canonical transfer matrices in equation (76) and (b) arbitrary transfer matrices.

Solving this equation one gets directly

$$c_1 = \frac{1}{\sqrt{1-|z_f|^2}} \exp(i\vartheta), \quad c_2 = -c_1 z_f^*, \quad (78)$$

and  $\vartheta$  is a real free parameter. The same procedure applies to matrices  $\hat{A}(\xi)$  and  $\hat{N}(\nu)$ .

The concept of orbit is especially appropriate for getting an intuitive picture of these actions. Given a point  $z$ , its orbit is the set of points  $z'$  obtained from  $z$  by the action of all the elements of the group. In figure 8.a we have plotted typical orbits for each one of the canonical forms  $\hat{K}(\phi)$ ,  $\hat{A}(\xi)$ , and  $\hat{N}(\nu)$ . They are

$$\begin{aligned} z' &= \Phi[\hat{K}(\phi), z] = z \exp(-i\phi), \\ z' &= \Phi[\hat{A}(\xi), z] = \frac{z - i \tanh(\xi/2)}{1 + iz \tanh(\xi/2)}, \\ z' &= \Phi[\hat{N}(\nu), z] = \frac{z + (1 + iz)\nu/2}{1 + (z - i)\nu/2}. \end{aligned} \quad (79)$$

For matrices  $\hat{K}(\phi)$  the orbits are circumferences centered at the origin and there are no invariant hyperbolic lines. For  $\hat{A}(\xi)$ , they are arcs of circumference going from the point  $+i$  to the point  $-i$  through  $z$  and they are known as hypercircles. Every hypercircle is equidistant [in the sense of the distance (70)] from the imaginary axis, which remains invariant (in the Euclidean plane the locus of a point at a constant distance from a fixed line is a pair of parallel lines). Finally, for  $\hat{N}(\nu)$  the orbits are circumferences passing through the point  $+i$  and joining the points  $z$  and  $-z^*$  and they are denominated horocycles: they can be viewed as the locus of a point that is derived from the point  $+i$  by a continuous parallel displacement (Coxeter, 1968).

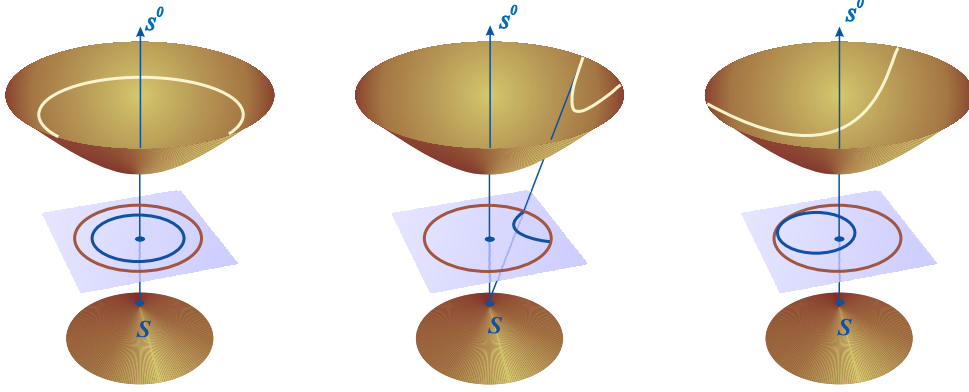


Figure 9: Unit hyperboloids defined in equation (38), representing the space of states for  $SO(2,1)$ . In each one of them we have plotted a typical orbit for the matrices  $\Lambda_{\hat{K}}$ ,  $\Lambda_{\hat{A}}$ , and  $\Lambda_{\hat{N}}$  (from left to right). In all the figures we have performed stereographic projection from the south pole  $S$  of the hyperboloid, to obtain the unit disk in the plane  $s^0 = 0$  and the corresponding orbits, which are the actions of the  $SU(1, 1)$  matrices.

For a general  $M_{ab}$  the corresponding orbits can be obtained by transforming with the appropriate matrix  $C$  the orbits delineated before. In figure 8.b we have plotted examples of such orbits for elliptic, hyperbolic, and parabolic actions. We stress that once the fixed points of the transfer matrix are known, one can ensure that  $z_a$  will lie in the orbit associated to  $z_b$ .

An alternative way to understand these results is to look at the canonical matrices in the Lorentz group  $SO(2, 1)$ . In fact, using (36) one finds that

$$\begin{aligned}\Lambda_{\hat{K}}(\phi) &= \begin{pmatrix} 1 & 0 & 0 \\ 0 & \cos \phi & \sin \phi \\ 0 & -\sin \phi & \cos \phi \end{pmatrix}, \\ \Lambda_{\hat{A}}(\xi) &= \begin{pmatrix} \cosh \xi & 0 & -\sinh \xi \\ 0 & 1 & 0 \\ -\sinh \xi & 0 & \cosh \xi \end{pmatrix}, \\ \Lambda_{\hat{N}}(\nu) &= \begin{pmatrix} 1 + (\nu^2/2) & \nu & -\nu^2/2 \\ \nu & 1 & -\nu \\ \nu^2/2 & \nu & 1 - (\nu^2/2) \end{pmatrix}.\end{aligned}\tag{80}$$

The action of these matrices in  $SO(2,1)$  is clear:  $\Lambda_{\hat{K}}(\phi)$  is a space rotation of angle  $\phi$  in the 1–2 plane,  $\Lambda_{\hat{A}}(\xi)$  is a boost in the direction of the axis 2 with velocity  $v = \tanh \xi$ ; and, finally,  $\Lambda_{\hat{N}}(\nu)$  is a space rotation of angle  $\tau_{\hat{N}}$  [such that  $\tan(\tau_{\hat{N}}) = \nu/2$ ] followed by a boost of angle  $\tau_{\hat{N}}$  and velocity  $v = \tanh(\nu/2)$ , both in the 1–2 plane. In figure 9 we have plotted examples of the orbits for each one of the subgroups in (80). For  $\Lambda_{\hat{K}}(\phi)$  the orbits are the intersection of the hyperboloid with planes  $s^0 = \text{constant}$ , for  $\Lambda_{\hat{A}}(\xi)$  with planes  $s^1 = \text{constant}$ , and for  $\Lambda_{\hat{N}}(\nu)$  with planes  $s^0 - s^2 = \text{constant}$ . Through stereographic projection we get the corresponding orbits for the matrices (76) in the unit disc.

#### 4.2. Transfer function in the half-plane

The unitary matrix (16) plays an important role in the intertwining between the two basic vector bases used for the transfer-matrix description. In mathematical terms,  $\mathcal{U}$  establishes a

one-to-one map between the groups  $SU(1, 1)$  and  $SL(2, \mathbb{R})$ . To investigate the meaning of this map we observe that if the point  $w \in \mathbb{C}$  is defined in terms of  $z$  by

$$w = \Phi[\mathcal{U}, z] = \frac{z+i}{1+iz}, \quad (81)$$

then the interior of  $\mathbb{D}$  is mapped onto the upper half-plane of the complex plane  $w$ , the boundary maps onto the real axis, while the exterior of  $\mathbb{D}$  becomes the lower half-plane. This remarkable map is known as the Cayley transform.

The metric now reads as

$$ds^2 = \frac{dw dw^*}{(\text{Im } w)^2}, \quad (82)$$

and the geodesic lines are the open semicircles orthogonal to the real axis. The Möbius transformations are

$$w_b = \Phi[\mathcal{M}_{ab}, w_a] = \frac{bw + c}{aw + d}, \quad (83)$$

with  $\mathcal{M}_{ab}$  obtained from  $M_{ab}$  through conjugation with  $\mathcal{U}$  as in equation (17). They are also isometries.

The points  $w$  in the upper half-plane constitute the Poincaré model of the hyperbolic plane  $\mathbb{H}$  (Stahl, 1993). In this way, one can transport all the geometrical properties of the unit disc  $\mathbb{D}$  to the upper half-plane  $\mathbb{H}$ .

Since the matrix conjugation does not change the trace, the same geometrical classification in three basic actions still holds. In fact, by conjugating with  $\mathcal{U}$  the canonical forms (76), the corresponding ones for  $SL(2, \mathbb{R})$  are

$$\begin{aligned} \hat{\mathcal{K}}(\phi) &= \begin{pmatrix} \cos(\phi/2) & \sin(\phi/2) \\ -\sin(\phi/2) & \cos(\phi/2) \end{pmatrix}, \\ \hat{\mathcal{A}}(\xi) &= \begin{pmatrix} e^{\xi/2} & 0 \\ 0 & e^{-\xi/2} \end{pmatrix}, \\ \hat{\mathcal{N}}(\nu) &= \begin{pmatrix} 1 & 0 \\ \nu & 1 \end{pmatrix}. \end{aligned} \quad (84)$$

These matrices have as fixed points  $+i$  (elliptic),  $0$  and  $\infty$  (hyperbolic), and  $\infty$  (parabolic), respectively. Clearly,  $\hat{\mathcal{K}}(\phi)$  is a rotation in phase space, also termed a fractional Fourier transform, while  $\hat{\mathcal{A}}$  is sometimes called a squeezer or hyperbolic magnifier: it scales the positive amplitude  $+$  up by the factor  $e^{\xi/2}$  and the negative one  $-$  down by the same factor. Finally,  $\hat{\mathcal{N}}(\nu)$  represents the action of a thin lens of power  $\nu$  (i.e., focal length  $1/\nu$ ) in geometrical optics (Wolf, 2004).

For the canonical forms (84), the orbits for a point  $w$  are

$$\begin{aligned} w' &= \frac{\cos(\phi/2)w - \sin(\phi/2)}{\sin(\phi/2)w + \cos(\phi/2)}, \\ w' &= e^{-\xi} w, \\ w' &= w + \nu. \end{aligned} \quad (85)$$

In figure 10.a we have plotted these orbits. For matrices  $\hat{\mathcal{K}}(\phi)$  they are circumferences centered at the invariant point  $+i$  and passing through  $w$  and  $-1/w$ . For  $\hat{\mathcal{K}}(\xi)$ , they are lines going

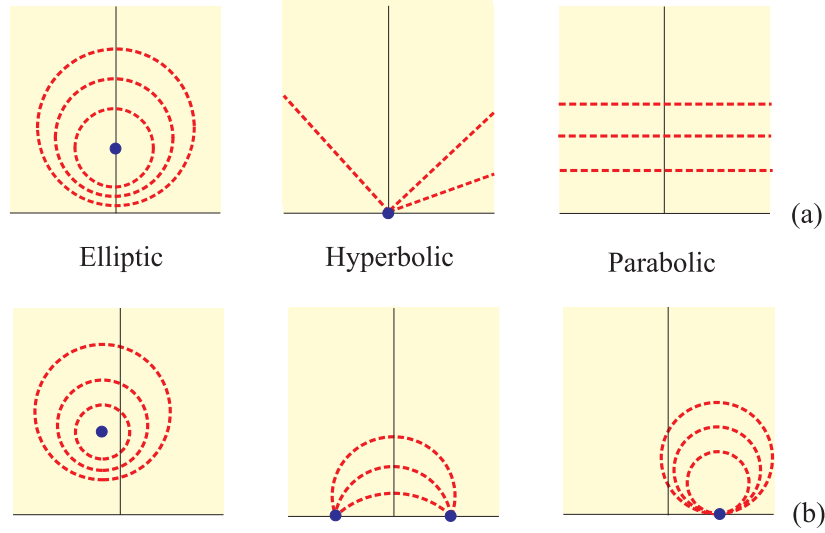


Figure 10: Plot of typical orbits in the hyperbolic plane  $\mathbb{H}$ : (a) canonical transfer matrices as in equation (84) and (b) arbitrary transfer matrices obtained by matrix conjugation.

from 0 to the  $\infty$  through  $w$  and they corresponds to hypercycles. Finally, for matrices  $\hat{N}(v)$  the orbits are lines parallel to the real axis passing through  $w$  and they are the horocycles (Coxeter, 1969). It is in the plane  $\mathbb{H}$  where the denomination of parallel displacements becomes manifest.

As we did before, for a general matrix  $M_{ab}$  the corresponding orbits can be obtained by transforming with the appropriate matrix  $C$  that transforms the fixed points of  $M_{ab}$  into the ones of  $\hat{K}(\phi)$ ,  $\hat{A}(\xi)$ , or  $\hat{N}(v)$ , respectively. In figure 10.b we have plotted typical examples of such orbits.

#### 4.3. Factoring the transfer matrix

Many types of factorizations have been considered in the literature (Arsenault and Macukow, 1983; Abe and Sheridan, 1994; Shamir and Cohen, 1995), all of them decomposing the matrix as a unique product of other matrices of simpler interpretation. Particularly, given the relevant role played by the Iwasawa decomposition, both in fundamental studies and in applications to several fields, one is tempted to investigate also its role in the transfer-matrix formalism.

Without embarking us in mathematical subtleties, the Iwasawa decomposition is established as follows (Barut and Rączka, 1977; Helgason, 1978): any element of a (noncompact semi-simple) Lie group can be written as an ordered product of three elements, taken one each from a maximal compact subgroup  $K$ , a maximal Abelian subgroup  $A$ , and a maximal nilpotent subgroup  $N$ . Furthermore, such a decomposition is global and essentially unique.

For a matrix  $M_{ab} \in \text{SU}(1, 1)$ , the decomposition reads as

$$M_{ab} = \hat{K}(\phi') \hat{A}(\xi') \hat{N}(v'), \quad (86)$$

where the matrices appearing here are of the form of the canonical ones in equation (76), but the parameters  $\phi'$ ,  $\xi'$ , and  $v'$  are given in terms of the elements  $\alpha$  and  $\beta$  of the transfer matrix by

$$\phi'/2 = \arg(\alpha + i\beta),$$

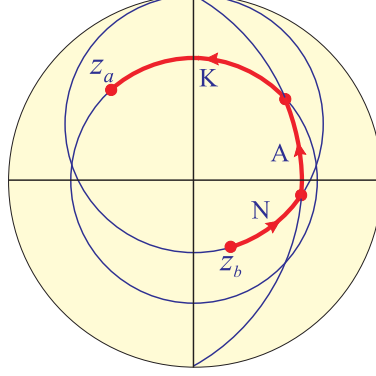


Figure 11: Representation in the unit disk of a transformation with the parameters indicated in the text. The point  $z_b$  is transformed by the system into  $z_a$ . The three orbits of the Iwasawa decomposition are indicated.

$$\begin{aligned}\xi'/2 &= \ln(1/|\alpha + i\beta|), \\ \nu'/2 &= \operatorname{Re}(\alpha\beta^*)/|\alpha + i\beta|^2.\end{aligned}\tag{87}$$

The importance of the Iwasawa decomposition reflects at the geometrical level: no matter how complicated a system is, its action can always be viewed in terms of these three basic actions with a patent meaning. Let us show this with a practical example: we consider a system that transforms the point  $z_b = 0.4 \exp(-i\pi/3)$  into  $z_a = -0.44 + 0.49i$  [see Monzón et al. (2002) for a realistic implementation]. In figure 11 we have plotted these points  $z_b$  and  $z_a$  in  $\mathbb{D}$ . Obviously, from these data alone we cannot infer at all the path for this discrete transformation.

The Iwasawa decomposition remedies this drawback: once we know the values of  $\phi'$ ,  $\xi'$ , and  $\nu'$  [that are easily computed from equation (87)] we get the intermediate values of  $z'$  for the ordered application of the matrices  $\hat{K}(\phi')$ ,  $\hat{A}(\xi')$ , and  $\hat{N}(\nu')$ , which, in fact, ensures that the trajectory from  $z_b$  to  $z_a$  is defined through the corresponding orbits, as shown in figure 11.

#### 4.4. Geometrical reflections as building blocks

In the Euclidean plane any isometry is either a rotation or a translation. In any case, reflections are the ultimate building blocks, since any isometry can be expressed as a composition of reflections. In this Euclidean plane, two distinct lines are either intersecting or parallel. Accordingly, the composition of two reflections in two intersecting lines forming an angle  $\phi$  is a rotation of angle  $2\phi$  around the intersection point, while the composition of two reflections in two parallel lines separated a distance  $d$  is a translation of value  $2d$ .

On the other hand, in hyperbolic geometry any two distinct lines are either intersecting (they cross in a point inside the unit disc), parallel (they meet at infinity; i.e., at a point on the boundary of the unit disc), or ultraparallel (they have no common points). A natural question arises: what is the composition of reflections in these three different kind of lines? To some extent, the answer could be expected: the composition is a rotation, a translation, or a parallel displacement, respectively. However, to gain further insights one needs to know how to deal with reflections in the unit disc.

In the Euclidean plane, given any straight line and a point  $P$  which does not lie on the line, its reflected image  $P'$  is such that the line is equidistant from  $P$  and  $P'$ . In other words, a reflection is a special kind of isometry in which the invariant points consist of all the points on the line.

The concept of hyperbolic reflection is completely analogous: given the hyperbolic line  $\ell$  and a point  $P$ , to obtain its reflected image  $P'$  in  $\ell$  we must drop a hyperbolic line  $\mathcal{L}$  from  $P$  perpendicular to  $\ell$  (such a hyperbolic line exists and it is unique) and extending an equal hyperbolic distance [according to (70)] on the opposite side of  $\mathcal{L}$  from  $P$ . In the unit disc, this corresponds precisely to the notion of an inversion.

We recall some facts about inversion (Coxeter, 1969). Let  $C$  be a circle with center  $\Omega$  and radius  $R$ . An inversion on the circle  $C$  maps the point  $z$  into the point  $z'$  along the same radius in such a way that the product of distances from the center  $\Omega$  satisfies

$$|z' - \Omega| |z - \Omega| = R^2, \quad (88)$$

and hence

$$z' = \Omega + \frac{R^2}{z^* - \Omega^*} = \frac{R^2 + \Omega z^* - \Omega^* \Omega}{z^* - \Omega^*}. \quad (89)$$

If the circle  $C$  is a hyperbolic line, it is orthogonal to the boundary of the unit disk and fulfills  $\Omega \Omega^* = R^2 + 1$ . In consequence

$$z' = \frac{\Omega z^* - 1}{z^* - \Omega^*}. \quad (90)$$

One can check (Pedoe, 1970) that inversion maps circles and lines into circles and lines, and transforms angles into equal angles (although reversing the orientation). If a circle  $C'$  passes through the points  $P$  and  $P'$ , inverse of  $P$  in the circle  $C$ , then  $C$  and  $C'$  are perpendicular. Moreover, the hyperbolic distance (70) is invariant under inversions. This confirms that inversions are indeed reflections and so they appear as the most basic isometries of the unit disc.

It will prove useful to introduce the conjugate bilinear transformation associated with a matrix  $M_{ab}$  as [compare with equation (68)]

$$z_a = \Phi^*[M_{ab}, z_b] = \frac{\alpha^* z_b^* + \beta^*}{\beta z_b^* + \alpha}. \quad (91)$$

With this notation we can recast equation (90) as

$$z' = \Phi^*[l_\Omega, z], \quad (92)$$

where the matrix  $l_\Omega \in \text{SU}(1, 1)$  associated to the inversion is (Barriuso et al., 2003b)

$$l_\Omega = \begin{pmatrix} -i \Omega^*/R & i/R \\ -i/R & i \Omega/R \end{pmatrix}. \quad (93)$$

The composition law for inversions can be stated as follows: if  $z' = \Phi^*[l_\Omega, z]$  and  $z'' = \Phi^*[l_{\Omega'}, z']$  then

$$z'' = \Phi[l_{\Omega'} l_\Omega^*, z]. \quad (94)$$

To appreciate the physical meaning of the inversion, assume that incoming and outgoing amplitudes are interchanged in the configuration shown in figure 1. This is tantamount to reversing the time arrow. It is known that for a right-traveling mover  $X_+$ , the conjugate amplitude  $[X_+]^*$  is a left phase-conjugate wave of the original one (Zel'dovich et al., 1985). In other words, the time-reversal operation can be viewed in this context as the transformation

$$z \mapsto \frac{1}{z^*}, \quad (95)$$



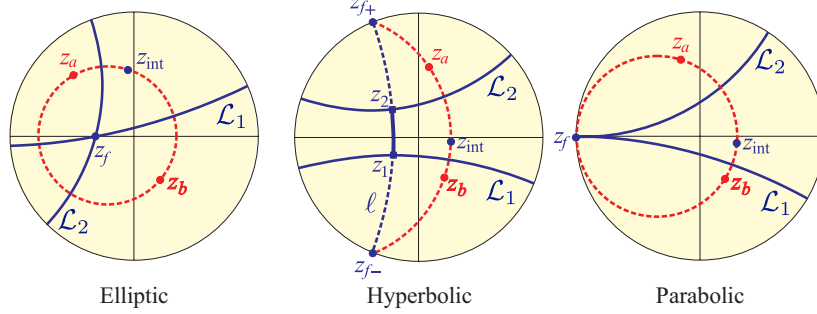


Figure 12: Decomposition of the transfer-matrix action in terms of two reflections for the elliptic, hyperbolic and parabolic cases.

for both  $a$  and  $b$ ; that is, it can be depicted by an inversion in the unit circle. The transformed points lie outside the unit circle because time reversal transforms the upper sheet into the lower sheet of the hyperboloid.

It is easy to convince oneself that the matrix relating these time-reversed amplitudes is precisely  $M_{ab}^*$  and so the action can be put as

$$(1/z_a)^* = \frac{\alpha^*(1/z_b)^* + \beta^*}{\beta(1/z_b)^* + \alpha}, \quad (96)$$

which expresses a general property of the time-reversal invariance.

In figure 12, we have drawn the three basic actions as a product of two reflections in two hyperbolic lines. For the elliptic case, the two hyperbolic lines  $\mathcal{L}_1$  and  $\mathcal{L}_2$  intersect at the fixed point  $z_f$  and form an angle  $\phi$ , which is just one half of the rotation angle. The first inversion maps  $z_b$  into the intermediate point  $z_{\text{int}}$ , which is mapped into  $z_a$  by the second inversion. Note that there are infinity pairs of lines satisfying these conditions, but chosen arbitrarily one of them, the other is uniquely determined. Once these lines are known, they delimit automatically the associated inversions.

For the hyperbolic case, there are no invariant points in the unit disc, but the hyperbolic line  $\ell$  joining the fixed points  $z_{f-}$  and  $z_{f+}$  is the axis of the hyperbolic translation. We have also plotted the hypercircle passing through  $z_b$  and  $z_a$ . The action can be now interpreted as the composition of two reflections in two ultraparallel hyperbolic lines  $\mathcal{L}_1$  and  $\mathcal{L}_2$  orthogonal to the translation axis. If  $\mathcal{L}_1$  and  $\mathcal{L}_2$  intersect the axis  $\ell$  at the points  $z_1$  and  $z_2$ , they must fulfill

$$d_H(z_b, z_a) = 2d_H(z_1, z_2), \quad (97)$$

in complete analogy with what happens in the Euclidean plane. Once again, there are infinity pairs of lines fulfilling this condition.

Finally, in the parabolic case, we have plotted the horocycle connecting  $z_b$  and  $z_a$  and the fixed point. Now, we have the composition of two reflections in two parallel lines  $\mathcal{L}_1$  and  $\mathcal{L}_2$  that intersect at the fixed point  $z_f$ , with the same constraints as before.

## 5. A closer look at the composition of transfer matrices

### 5.1. Setting up the inverse system

The property (19) has allowed us to characterize a compound system, as expressed more explicitly in (29). In its simplest form, it states that given two potentials  $V_1$  and  $V_2$ , described by the transfer matrices  $M_1$  and  $M_2$ , with scattering amplitudes  $(r_1, t_1)$  and  $(r_2, t_2)$ , respectively (once more we drop the subscript  $ab$  to simplify the notation), the action of the compound system is

$$M_{12} = M_1 M_2, \quad (98)$$

and the reflection and transmission amplitudes associated to  $M_{12}$  are

$$r_{12} = \frac{r_1 + r_2 \exp(i2\tau_1)}{1 + r_1^* r_2 \exp(i2\tau_1)}, \quad t_{12} = \frac{t_1 t_2}{1 + r_1^* r_2 \exp(i2\tau_1)}, \quad (99)$$

with the same notation as in equation (44). With a bit of effort, one can derive valuable bounds on these coefficients (Visser, 1999; Boonserm and Visser, 2010a).

According to the general form (7), the identity matrix has unit transmission and zero reflection coefficients. In other words, it represents an antireflection system (without transmission phase shift). In consequence, two systems that are inverse, when composed give an antireflection system.

Let us investigate the outstanding example of a single potential barrier of width  $L_1$  and height  $V_0$ . For the time being, we take  $E > V_0$ . Consequently, we look for another barrier of the same height such that, when put together with the original, gives the identity transfer matrix.

A simple glance at the coefficients in (9), reveals two possibilities. The first is to couple other barrier with the same wave number  $\kappa$  and width  $L_2$  such that

$$\sin[\kappa(L_1 + L_2)] = 0, \quad (100)$$

in such a way that the resulting barrier presents a transmission resonance. The second solution is to use a “complementary” barrier; that is, one having the same length and height, but opposite wave number  $-\kappa$ , so it acts as canceling the effects of the first.

Our geometrical picture leads to an appealing interpretation of these facts. In figure 13 we have schematized the action of the original barrier as a rotation of angle  $\varphi_1$  around the fixed points. The two previous solutions are a rotation of angle  $2\pi - \varphi_1$  and a rotation of angle  $-\varphi_1$ , respectively, getting thus the identity in two different ways.

The barrier can be seen as a quantum analog of a layer in classical optics. The condition  $E > V_0$  ensures the classical regime in which light striking the layer is partly reflected and partly transmitted. On the contrary,  $E < V_0$  corresponds to an imaginary refractive index, producing total internal reflection (Bohm, 1989). So, the condition  $E > V_0$  prevents the appearance of total reflection.

Negative values of the wave vector  $\kappa$  can be realized in terms of negative effective particle mass  $m$  (Kobayashi, 2006; Dragoman and Dragoman, 2007). The analog phenomenon in optics is a medium with both negative electrical permittivity  $\epsilon$  and magnetic permeability  $\mu$ . This is at the center of a lively and sometimes heated debate (Cai and Shalaev, 2009). This idea dates back to 1968, when Veselago (1968) theoretically predicted that these remarkable materials would exhibit a number of unusual effects derived from the fact that in them the vectors  $(\mathbf{k}, \mathbf{E}, \mathbf{B})$  of a plane wave form a left-handed (LH) rather than a right-handed (RH) set. For this reason, he

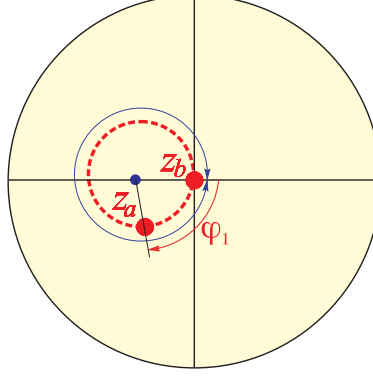


Figure 13: Rotation in the unit disk associated with a potential barrier described by the transfer matrix  $M_1$  transforming the point  $z_b = 0$  into  $z_a = r_1$  with the scattering amplitudes ( $r_1 = -0.3804 - i0.3339i$ ,  $t_1 = 0.5689 - i0.6482$ ). The orbits associated with the two solutions in the text can be either clockwise (of angle  $2\pi - \varphi_1$ ) or counterclockwise (of angle  $\varphi_1$ ) to give the identity.

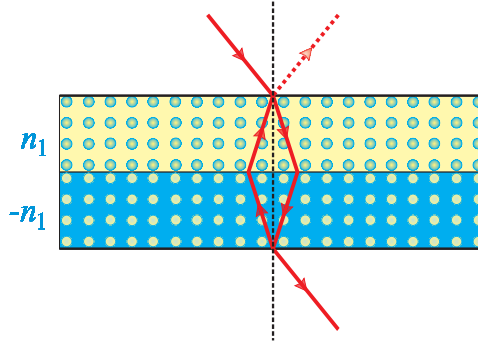


Figure 14: Scheme of the energy flow for the system resulting by putting together two identical slab, one made of RH and other of LH material. Both constitute a pair of complementary media, each canceling the effect of the other. Consequently, no reflection occurs, as indicated by the dotted line.

called them LH media. One of the most interesting properties of these LH materials is a negative refraction at the interface with a RH medium. Our solution for complementary barriers can be interpreted as putting together two RH and LH slabs (Monzón et al., 2006, 2008). The scheme of the energy flow in the resulting system appears in figure 14.

The discussion so far admits a straightforward generalization for any arbitrary potential. Indeed, let  $M_{ab}$  be the transfer matrix of a potential that can be decomposed in an arbitrary number of barriers (some having positive and some negative values of the wave vector  $\kappa$ ), which can be constructed by a direct extension of (29). Now, we take the potential in the reverse order, which is represented by  $M_{ba}$  in (8). Next, either we complete every barrier as in equation (100) or we switch every barrier with positive  $\kappa_j$  to an identical one with negative  $\kappa_j$  and viceversa. In both cases, this new system is represented by  $M_{ba}^*$ . Since one can check that

$$M_{ba}^* = M_{ab}^{-1}, \quad (101)$$

when both systems are put together they give the identity.

This substitution  $\kappa_j \mapsto -\kappa_j$  formalizes in a different framework the notion of “complementary” media introduced by Pendry and Ramakrishna (2003): any medium can be optically cancelled by an equal thickness of material constructed to be an inverted mirror image of the medium, with  $\epsilon$  and  $\mu$  reversed in sign. That is, complementary media cancel one another and become invisible (i.e., a perfect antireflector).

### 5.2. The Wigner angle

In special relativity there is an intriguing phenomenon that emerges in the composition of two noncollinear pure boosts: the combination of two such successive boosts cannot result in a pure boost, but renders an additional rotation, usually known as the Wigner rotation (Wyk, 1984; Ben-Menahem, 1985; Strandberg, 1986; Aravind, 1997; Ungar, 2001; Malykin, 2006; O’Donnell and Visser, 2011) [sometimes the name of Thomas rotation (Jackson, 1975; Ungar, 1989; Muller, 1992; Hamilton, 1996) is also used]. In other words, boosts are not a subgroup.

To fix the physical background, consider three reference frames  $K$ ,  $K'$  and  $K''$  (see figure 15). Frames  $K$ - $K'$  and  $K'$ - $K''$  have parallel respective axes. Frame  $K''$  moves with uniform velocity  $\vec{v}_2$  with respect to  $K'$ , which in turn moves with velocity  $\vec{v}_1$  relative to  $K$ . The Lorentz transformation  $\Lambda_{12}$  that connects  $K$  with  $K''$  is given by the product  $L_1 L_2$ , which can be decomposed as

$$L_1 L_2 = \Lambda_{12} = R(\psi) L_{(12)}. \quad (102)$$

An equivalent decomposition in terms of a boost with the same modulus of  $\vec{v}_{12}$  but with a different direction postmultiplied by the same rotation is also possible (Ungar, 1989; Aravind, 1997).

In words, this means that an observer in  $K$  sees the axes of  $K''$  rotated relative to the observer’s own axes by a Wigner rotation  $R(\psi)$ . More explicitly, it is possible to show that the axis  $\hat{n}$  and angle  $\psi$  of this rotation are (Ben-Menahem, 1985; Malykin, 2006; Ritus, 2008)

$$\hat{n} = \frac{\vec{v}_2 \times \vec{v}_1}{|\vec{v}_2 \times \vec{v}_1|}, \quad \tan(\psi/2) = \frac{\sin \Theta}{K + \cos \Theta}, \quad (103)$$

where  $\Theta$  is the angle between  $\vec{v}_1$  and  $\vec{v}_2$ , and

$$K^2 = \frac{\gamma_1 + 1}{\gamma_1 - 1} \frac{\gamma_2 + 1}{\gamma_2 - 1} = \frac{1}{\tanh^2(\zeta_1/2) \tanh^2(\zeta_2/2)}, \quad (104)$$

$\gamma_1$  and  $\gamma_2$  being the corresponding factors for  $\vec{v}_1$  and  $\vec{v}_2$ , while  $\zeta_1$  and  $\zeta_2$  are the rapidities. This means that  $\tan(\psi/2)$  depends on the velocities as  $v_1 v_2$ , so the Wigner rotation is a second-order effect and is absent in the non-relativistic limit.

On the other hand, the resulting boost  $L_{(12)}$  has a velocity fulfilling

$$\gamma_{12} = \gamma_1 \gamma_2 (1 + \vec{v}_1 \cdot \vec{v}_2) = \gamma_1 \gamma_2 (1 + v_1 v_2 \cos \Theta), \quad (105)$$

while the direction of  $\vec{v}_{12}$  has a complicated expression of little interest here.

The set of boosts could be regarded as a hyperbolic space provided the velocity  $v$  is replaced by the hyperbolic parameter  $\zeta = \tanh^{-1}(v)$ , which constitutes the usual rapidity space and whose line element has a Lobachevskian metric, as known from long times ago (Landau and Lifshitz, 2000; Rhodes and Semon, 2004). A triangle in this rapidity space obeys a non-Euclidean geometry and, in our context, this results in the fact that the parameters (105) of the compound boost  $L_{(12)}$  can be recast as

$$\cosh \zeta_{12} = \cosh \zeta_1 \cosh \zeta_2 + \sinh \zeta_1 \sinh \zeta_2 \cos \Theta, \quad (106)$$

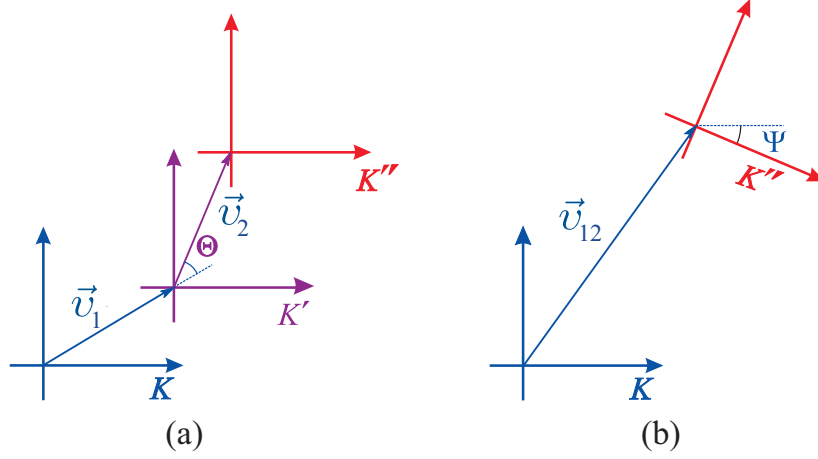


Figure 15: (a) Reference frame  $K''$  moves with velocity  $\vec{v}_2$  relative to frame  $K'$  while frame  $K'$  moves with velocity  $\vec{v}_1$  relative to frame  $K$ . (b) The axes of  $K''$  appears rotated relative to  $K$  by the Wigner angle  $\Theta$ . Time and one space dimension are suppressed for clarity.

which is nothing but the hyperbolic law of cosines for the triangle induced by the boosts  $L_1$ ,  $L_2$ , and  $L_{(12)}$ . Therefore, given two sides and the included angle of the triangle (corresponding to the two non-collinear boosts we wish to combine) one can determine the third side and its angle by a simple use of hyperbolic trigonometry.

Moreover, a standard calculation shows that the expression (103) for the Wigner angle  $\psi$  gives precisely the area of this triangle (Chen and Ge, 1998). We recall that for a hyperbolic (spherical) triangle the sum of the angles is less (greater) than  $\pi$  with the angular defect (excess) being the area.

This suggests to look at the Wigner angle as a geometric phase. Roughly speaking, geometric phases are associated with the cyclic evolution of a system and the crucial concept to their understanding is anholonomy. Anholonomy (Shapere and Wilczek, 1989) is a phenomenon in which non-integrability causes some variables to fail to return to their original values when others, which drive them, are altered round a cycle (the simplest example occurs in the parallel transport of vectors). This behaviour was anticipated by Pancharatnam when discussing the phase shift that appears in the coherent addition of two polarized beams on the Poincaré sphere.

It is worth mentioning that geometric phases associated with the group  $SU(1,1)$  have been previously identified (Simon and Mukunda, 1993a; Monzón and Sánchez-Soto, 1999, 2001). The idea is to view the rapidity triangle as imbedded in the unit hyperboloid, which is a manifold of constant negative curvature (of value  $-1$ ). The analogous triangle for rotations instead of boosts is traced on the unit sphere (of curvature  $+1$ ) and the geometric phase appears as the area enclosed by the triangle on the sphere (Levi, 1994). Thus, it is tempting to infer that the Wigner angle is just the area of the triangle on the hyperboloid, with the opposite sign to that of rotations: in fact, this is true as proved by Aravind (1997) and others (Jordan, 1988; Urbantke, 1990).

After our discussion in the previous section, it is clear that the problem should arise in the context of transfer matrices. First of all, it is worth emphasizing that the two combining boosts and the resulting one are in the same plane, usually assumed for simplicity to be the 1-2 plane.

In consequence, we restrict our attention to the composition of two Hermitian matrices  $H_1$

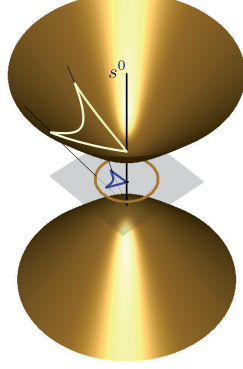


Figure 16: Geodesic triangle in the unit disk for the potentials indicated in the text. By stereographic projection the associated triangle is also plotted in the unit hyperboloid.

and  $H_2$  for, as explained before, they are the equivalent to pure boosts. In complete analogy with equation (102) we have now

$$H_1 H_2 = M_{12} = UH_{(12)} = \begin{pmatrix} \exp(-i\psi/2) & 0 \\ 0 & \exp(i\psi/2) \end{pmatrix} \times \frac{1}{|t_{12}|} \begin{pmatrix} 1 & r_{12}^* \exp(i\psi) \\ r_{12} \exp(-i\psi) & 1 \end{pmatrix}, \quad (107)$$

where  $r_{12}$  and  $t_{12}$  are given by (99) and

$$\psi = 2 \arg t_{12} = \arg(1 + r_1 r_2^*). \quad (108)$$

The appearance of an extra unitary matrix is the signature of a Wigner rotation and, accordingly, the Wigner angle  $\psi$  viewed in  $SO(2,1)$  is just twice the phase of the transmission coefficient of the compound system. Obviously, when  $\rho_1 = \rho_2$ , the Wigner rotation is absent, since then we are dealing with two parallel boosts, whose composition leads to the famous Einstein addition law of velocities (Vigoureux, 1992; Vigoureux and Grossel, 1993).

To show an explicit implementation of this phenomenon (Monzón and Sánchez-Soto, 2001), we take two potentials with Hermitian transfer matrices  $H_1$  and  $H_2$ , and scattering coefficients ( $r_1 = 0.3736 - i0.2014$ ,  $t_1 = 0.9055$ ) and ( $r_2 = 0.3413i$ ,  $t_2 = 0.9399$ ). Equation (107) fixes a third potential  $H_{(12)}^{-1}$  such that when put together the compound system is an antireflection system with phase in transmission equal to the Wigner angle. This is shown in figure 16, where the triangle is also plotted in the unit hyperboloid.

### 5.3. Hyperbolic turns

According to Hamilton (1853), the turn associated with a rotation of axis  $\hat{n}$  and angle  $\vartheta$  is a directed arc of length  $\vartheta/2$  on the great circle orthogonal to  $\hat{n}$  on the unit sphere. By means of these objects, the composition of rotations is described through a parallelogram-like law: if these turns are translated on the great circles until the head of the arc of the first rotation coincides with the tail of the arc of the second one, then the turn between the free tail and the head is associated with the resultant rotation (Biedenharn and Louck, 1981). Hamilton turns are thus analogous for spherical geometry to sliding vectors in Euclidean geometry. It is unfortunate that this elegant idea of Hamilton is not as widely known as it rightly deserves.

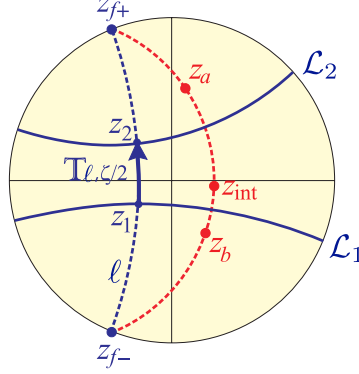


Figure 17: Representation of the sliding turn  $\mathbb{T}_{\ell, \zeta/2}$  in terms of two reflections in two lines  $\mathcal{L}_1$  and  $\mathcal{L}_2$  orthogonal to the axis of the translation  $\ell$ , which has two fixed points  $z_{f-}$  and  $z_{f+}$ . The transformation of a typical off axis point  $z_b$  is also shown.

The purpose of this section is to show how the use of turns affords an intuitive and visual image of all problems involved in quantum scattering and reveals the emergence of hyperbolic geometry in the composition law of transfer matrices.

Let us focus on the case of  $|\text{Tr}(\mathbf{M})| > 2$ . This is not a serious restriction, since any matrix of  $\text{SU}(1, 1)$  can be written (in many ways) as the product of two hyperbolic translations (Juárez and Santander, 1982; Simon et al., 1989a; Sánchez-Soto et al., 2005; Simon et al., 2006). The axis of the hyperbolic translation is the geodesic line joining the two fixed points.

As explained in section 4.4, any pair of points  $z_1$  and  $z_2$  on the axis of the translation  $\ell$  at a distance  $\zeta/2$  can be chosen as intersections of  $\mathcal{L}_1$  and  $\mathcal{L}_2$  (orthogonal lines to  $\ell$ ) with  $\ell$ . It is natural to associate to the translation an oriented segment of length  $\zeta/2$ , with

$$\zeta = d_{\text{H}}(z_b, z_a), \quad (109)$$

but otherwise free to slide on  $\ell$  (see figure 17). This is analogous to Hamilton's turns, and will be called a hyperbolic turn  $\mathbb{T}_{\ell, \zeta/2}$  (Simon et al., 1989b).

Using this construction, an off-axis point such as  $z_b$  will be mapped by these two reflections (through an intermediate point  $z_{\text{int}}$ ) to another point  $z_a$  along a curve equidistant to the axis. These other curves, unlike the axis of translation, are not hyperbolic lines. What matters is that once the turn is known, the transformation of every point in the unit disk is automatically established.

Alternatively, we can formulate the concept of turn as follows. Let  $\mathbf{M}$  be a hyperbolic translation with  $\text{Tr}(\mathbf{M})$  positive [equivalently,  $\text{Re}(\alpha) > 1$ ]. Then,  $\mathbf{M}$  is positive definite and one can ensure that its positive square root exists and reads as (Barriuso et al., 2004)

$$\sqrt{\mathbf{M}} = \frac{1}{\sqrt{\text{Tr}(\mathbf{M}) + 2}} \begin{pmatrix} \alpha + 1 & \beta \\ \beta^* & \alpha^* + 1 \end{pmatrix}. \quad (110)$$

This matrix has the same fixed points as  $\mathbf{M}$ , but the translated distance is just half the induced by  $\mathbf{M}$ ; i.e., we set

$$\zeta(\mathbf{M}) = 2\zeta(\sqrt{\mathbf{M}}). \quad (111)$$

This suggests that the matrix  $\sqrt{\mathbf{M}}$  can be appropriately associated to the turn  $\mathbb{T}_{\ell, \zeta/2}$  that represents

the translation induced by  $M$ . Therefore, we symbolically write

$$\mathbb{T}_{\ell, \zeta/2} \mapsto \sqrt{M}. \quad (112)$$

Let  $\zeta_1$  and  $\zeta_2$  be the corresponding translated distances along intersecting axes  $\ell_1$  and  $\ell_2$ , respectively. Take now the associated turns  $\mathbb{T}_{\ell_1, \zeta_1/2}$  and  $\mathbb{T}_{\ell_2, \zeta_2/2}$  and slide them along  $\ell_1$  and  $\ell_2$  until they are “head to tail”. Afterwards, the turn determined by the free tail and head is the turn associated to the resultant, which can be interpreted as a translation of parameter  $\zeta_{12}$  along the line  $\ell_{12}$ .

This construction is illustrated in figure 18, where the pertinent parameters are  $(r_1 = 0.3103 - i0.8274, t_1 = 0.4383 + i0.1644)$  and  $(r_2 = 0.6820 + i0.3079, t_2 = 0.6601 - i0.0659)$ . The application of (99) gives  $(r_{12} = 0.5210 - i0.7331, t_{12} = 0.3915 - i0.1947)$ . The noncommutative character is evident, and can also be inferred from the obvious fact that  $M_{12} \neq M_{21}$ .

In Euclidean geometry, the resultant of this parallelogram law can be quantitatively determined by a direct application of the cosine theorem. For any hyperbolic triangle with sides of lengths  $\zeta_1$  and  $\zeta_2$  that make an angle  $\Theta$ , the expression is precisely given in equation (106).

## 6. Periodic systems

### 6.1. Finite periodic structures

Periodic potentials are those whose shape is repeated indefinitely with period  $d$ ; i.e.,  $V(x) = V(x + d)$ . The distinctive feature of these potentials is that the frequencies fall into continuous bands, separated by forbidden gaps. In the quantum context this was first noted by Kronig and Penney (1931) in the classic paper that laid the foundation for the modern theory of solids. This band structure also occurs, in principle, for mechanical, acoustical, and electromagnetic waves (Griffiths and Steinke, 2001).

There is a recurring interest in the related instance where the potential  $V(x)$  consists of a finite number (say  $N$ ) of identical cells. We shall call that situation a finite periodic structure (the term locally periodic is also employed); such potentials are produced by any finite lattice and they are of great importance for a number of applications, such as superlattices, photonic crystals, multilayers, etc, where the finite size must unavoidably be taken into account (Felbacq et al., 1998; Busch et al., 2007).

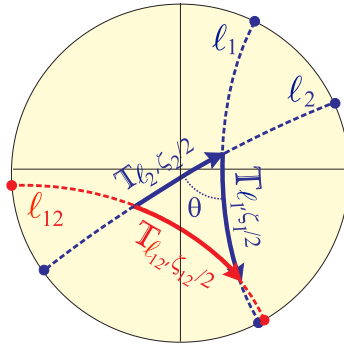


Figure 18: Composition of two hyperbolic turns  $\mathbb{T}_{\ell_1, \zeta_1/2}$  and  $\mathbb{T}_{\ell_2, \zeta_2/2}$  by using a parallelogramlike law when the axes  $\ell_1$  and  $\ell_2$  of the translations intersect.



From a theoretical standpoint finite periodic systems are more difficult to analyze because Bloch theorem (Ashcroft and Mermin, 1976), which so dramatically simplifies the periodic problem, does not apply. It is amazing that the finite periodic case can be solved analytically for arbitrary  $N$ . This was first discovered by Abelès (1948) and rediscovered in the quantum context by Kiang (1974) and Cvetič and Pičman (1981) and later by several others (Vezzetti and Cahay, 1986; Lee et al., 1989; Kalotas and Lee, 1991; Griffiths and Taussig, 1992; Sprung et al., 1993; Wu et al., 1993; Rozman et al., 1994b; Livioti, 1994; Chuprikov, 1996; Erdős et al., 1997; Barra and Gaspard, 1999; Sprung et al., 1999; Morozov et al., 2002; Pereyra and Castillo, 2002).

Let us suppose that the arbitrary potential  $V(x)$  (the basic unit cell) is replicated  $N$  times at regular intervals, as schematized in figure 19. Our problem is to construct the transfer matrix for the whole array, given the transfer matrix  $M$  for the single cell. The amplitudes at the  $j$ th cell are

$$\begin{pmatrix} A_{+,j} \\ A_{-,j} \end{pmatrix} = M \begin{pmatrix} B_{+,j+1} \\ B_{-,j+1} \end{pmatrix}. \quad (113)$$

Using this equation recursively we have that

$$\begin{pmatrix} A_{+,0} \\ A_{-,0} \end{pmatrix} = M^N \begin{pmatrix} B_{+,N} \\ B_{-,N} \end{pmatrix}, \quad (114)$$

so the whole problem reduces to the evaluation of  $M^N$ . There are several elegant ways of calculating this power. Perhaps, the most efficient is to use the Cayley-Hamilton theorem, which states that any square matrix satisfies its own characteristic equation (Gantmacher, 2000). This means that

$$M^2 - 2uM + \mathbb{1} = 0. \quad (115)$$

where  $u = [\text{Tr}(M)]/2$ . Consequently, any higher power of  $M$  can be reduced to a linear combination of  $M$  and the identity  $\mathbb{1}$ . By induction, we obtain the expression

$$M^N = U_{N-1}(u)M - U_{N-2}(u)\mathbb{1}. \quad (116)$$

Here

$$U_N(\theta) = \frac{\sin[(N+1)\theta]}{\sin\theta}, \quad (117)$$

with  $\cos\theta = u$ , are the Chebyshev polynomials of the second kind satisfying the recursion relation (Abramowitz and Stegun, 1996)

$$U_{N+1} = 2uU_N + U_{N-1}, \quad N \geq 1, \quad (118)$$

and  $U_0(u) = 1$ ,  $U_1(u) = 2u$ . This provides a closed solution to the problem; in particular, for incidence from the left the reflectance  $\mathcal{R} = |r|^2$  of the array is

$$\mathcal{R}^{(N)} = \frac{[|\beta|U_{N-1}(u)]^2}{1 + [|\beta|U_{N-1}(u)]^2}, \quad (119)$$

which requires to know the transfer matrix for the unit cell.

The Chebyshev polynomials play, for finite systems, a similar role to the one played by Bloch functions in the description of infinite periodic systems. In addition, they are very useful to perform numerical calculations. However, it is not easy to separate the different behaviors according to the value of the trace, as it happens for infinite periodic media. For this reason, we will follow an alternative route based on geometrical properties.

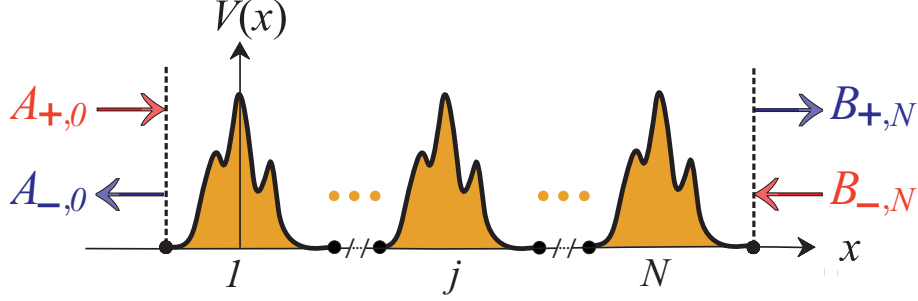


Figure 19: A finite periodic potential constructed from the basic cell  $V(x)$ .

## 6.2. Bandgaps in the unit disc

First, we note that the reflectance associated to each one of the canonical matrices (76) is

$$\begin{aligned}\mathcal{R}_{\hat{K}} &= 0, \\ \mathcal{R}_{\hat{A}} &= \tanh^2(\xi/2), \\ \mathcal{R}_{\hat{N}} &= (\nu/2)^2/[1 + (\nu/2)^2].\end{aligned}\tag{120}$$

While  $\mathcal{R}_{\hat{K}}$  is identically zero,  $\mathcal{R}_{\hat{A}}$  and  $\mathcal{R}_{\hat{N}}$  tend to unity when  $\xi$  and  $\nu$ , respectively, increase. Nevertheless, they have distinct growths:  $\mathcal{R}_{\hat{A}}$  goes to unity exponentially, while  $\mathcal{R}_{\hat{N}}$  goes as  $O(\nu^{-2})$ .

Let  $C$  be the matrix (74) that goes by conjugation from an arbitrary  $M$  to its canonical version. All the subgroups generated by  $\hat{K}(\phi)$ ,  $\hat{A}(\xi)$ , or  $\hat{N}(\nu)$  are one-parametric and therefore Abelian, so we have that

$$\hat{M}(\mu_1)\hat{M}(\mu_2) = \hat{M}(\mu_1 + \mu_2),\tag{121}$$

where  $\mu$  is the appropriate parameter  $\phi$ ,  $\xi$ , or  $\nu$ . For an  $N$ -cell system the overall transfer matrix is

$$C^{-1} [\hat{M}(\mu)]^N C = C^{-1} \hat{M}(N\mu) C,\tag{122}$$

From this equation, one must expect three universal behaviors of the reflectance according the transfer matrix for the basic cell is elliptic, hyperbolic, or parabolic. We shall work in what follows the detailed structure of these three basic laws.

Since the stop bands are given by the condition  $|\text{Tr}(M)| > 2$ , we first consider the case when  $M$  is hyperbolic. We can rewrite equation (73) as

$$M = C^{-1} A(\xi) C,\tag{123}$$

and  $\xi$  is given by  $\text{Tr}(M) = 2 \cosh \xi > 2$ , because we are taking into account only positive values of  $\text{Tr}(M)$ . One solution of equation (123) is (Monzón et al., 2003)

$$c_1 = F(\beta^* + i \sinh \xi), \quad c_2 = -iF \text{Im}(\alpha),\tag{124}$$

with  $F = 1/\sqrt{2 \sinh \xi [\sinh \xi - \text{Im}(\beta)]}$ .

Carrying out the matrix multiplications in (122) it is easy to compute the reflectance:

$$\mathcal{R}_A^{(N)} = \frac{|\beta|^2}{|\beta|^2 + [\sinh(\xi)/\sinh(N\xi)]^2}.\tag{125}$$

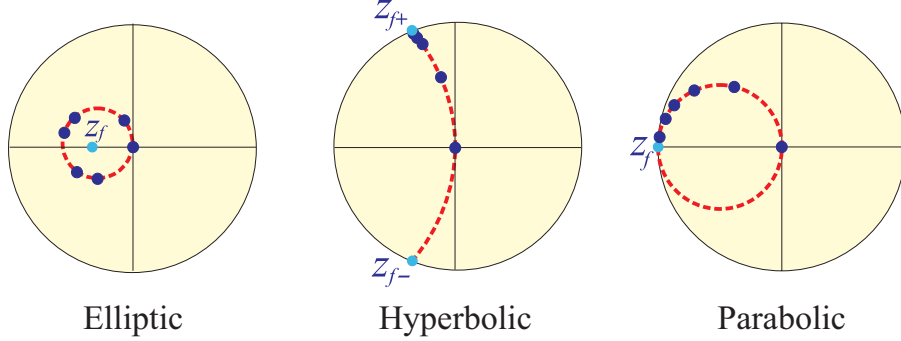


Figure 20: Successive iterates ( $N = 1, \dots, 5$ ) for an elliptic, hyperbolic, and parabolic action starting from the origin as the initial point. The fixed points are marked in cyan. Only hyperbolic and parabolic actions tend to the unit circle.

This is an exact expression for any value of  $N$ . As  $N$  grows,  $\mathcal{R}_A^{(N)}$  approaches unity exponentially, as expected from a stop band.

The band edges are determined by  $|\text{Tr}(\mathbf{M})| = 2$ ; that is, when  $\mathbf{M}$  is parabolic. A calculation very similar to the previous one shows that

$$\mathcal{R}_N^{(N)} = \frac{|\beta|^2}{|\beta|^2 + (1/N)^2}, \quad (126)$$

with a typical behavior  $\mathcal{R}_N^{(N)} \sim 1 - O(N^{-2})$  that is universal in the physics of reflection. The general results (125) and (126) have been obtained in a different framework by Yeh (1988) and Lekner (1994).

Finally, in the allowed bands we have  $|\text{Tr}(\mathbf{M})| < 2$ ,  $\mathbf{M}$  is elliptic, and

$$\mathcal{R}_K^{(N)} = \frac{Q^2 - 2Q \cos(2N\Xi)}{1 + Q^2 - 2Q \cos(2N\Xi)}, \quad (127)$$

where

$$Q = \frac{|\beta|^2}{|\beta|^2 - |\alpha - e^{i\Xi}|^2}, \quad e^{i\Xi} = \text{Re}(\alpha) + i \sqrt{1 - [\text{Re}(\alpha)]^2}. \quad (128)$$

Now the reflectance oscillates with  $N$  between the values  $(Q^2 - 2Q)/(Q - 1)^2$  and  $(Q^2 + 2Q)/(Q + 1)^2$ .

It seems quite pertinent to picture these behaviors in the unit disc. Note that if we have only an incident wave from the left ( $B_- = 0$ ; that is,  $z_b = 0$ ) and simultaneously  $|z_a| = 1$  the system behaves as a perfect mirror. Therefore, a mirror maps the origin into a point on the unit circle.

Henceforth, we shall take  $z_0 \equiv z_b = 0$ . As mentioned before, all the points  $z_N$  obtained by iteration from  $z_0$  lie in the orbit associated to the initial point  $z_0$  by the single cell, which is determined by its fixed points.

In figure 20 we have plotted the successive iterates worked out numerically for the three archetypical actions (Barriuso et al., 2003a). In the elliptic case, the points  $z_N$  revolve in the orbit centered at the fixed point and the system never reaches the unit circle. On the contrary, for the hyperbolic and parabolic actions the iterates converge to one of the fixed points on the unit circle, although with different laws, which correspond to the stop band and edges, respectively (Lekner, 2000).

The  $N$ th iterate can be easily computed for the canonical forms in equation (76) and then, conjugating as in (73). For a hyperbolic action one has

$$z_N = \frac{1 - \xi^N}{1 - \xi^N(z_{f+}/z_{f-})} z_{f+}, \quad (129)$$

where  $\xi = (\alpha + \beta z_{f-})/(\alpha + \beta z_{f+})$  is a complex number satisfying  $|\xi| < 1$  and  $z_{f\pm}$  are the fixed points. Analogously, for the parabolic case we have

$$z_N = \frac{N\beta z_f^2}{N\beta z_f - 1}, \quad (130)$$

$z_f$  being the (double) fixed point. In both cases,  $z_N$  converges to one of the fixed points on the unit circle, so  $|z_N| \rightarrow 1$  when  $N$  increases, a typical behavior of a stop band (or, in other terms, a perfect mirror). In the mathematical literature this limit point is referred to as the Denjoy-Wolff point of the map (Kapeluszny et al., 1999).

### 6.3. Bandgaps in the half-plane

The previous formalism can be translated to the hyperbolic half-plane  $\mathbb{H}$  by the unitary transformation (16), as explained in section 4.2. However, to give a physical feeling, we prefer to illustrate this point with the simple yet interesting case of optical beams (Barriuso et al., 2005a).

In paraxial-wave optics, axially symmetric (monochromatic scalar) beams are specified in the Hilbert space of complex-valued square-integrable wave-amplitude functions  $\Psi(x)$  (Gloge and Marcuse, 1969), with  $x$  labeling the axis. To deal with partially coherent beams we specify the field not by its amplitude, but by its cross-spectral density. The latter is defined in terms of the former as

$$\Gamma(x_1, x_2) = \langle \Psi^*(x_1) \Psi(x_2) \rangle, \quad (131)$$

where the angular brackets denote ensemble averages.

There is a wide family of beams, the Schell-model fields (Wolf and Collett, 1978; Foley and Zubairy, 1978; Starikov and Wolf, 1982; Friberg and Sudol, 1982; Gori, 1983; Gori and Grella, 1984; Friberg and Turunen, 1988; Ambrosini et al., 1994), for which the cross-spectral density (131) factors in the form

$$\Gamma(x_1, x_2) = \sqrt{I(x_1)I(x_2)} \mu(x_1 - x_2). \quad (132)$$

Here  $I$  is the intensity distribution and  $\mu$  is the normalized degree of coherence, which is translationally invariant. When these two fundamental quantities are Gaussians

$$I(x) = \frac{I}{\sqrt{2\pi}\sigma_I} \exp\left(-\frac{x^2}{2\sigma_I^2}\right), \quad \mu(x) = \exp\left(-\frac{x^2}{2\sigma_\mu^2}\right), \quad (133)$$

the beam is said to be a Gaussian Schell model (GSM). Here,  $I$  is a constant independent of  $x$  that can be identified with the total irradiance and  $\sigma_I$  and  $\sigma_\mu$  are, respectively, the effective beam width and the transverse coherence length. Other well-known families of Gaussian fields are special cases of these GSM fields: when  $\sigma_\mu \ll \sigma_I$  we have the Gaussian quasihomogeneous field, and when  $\sigma_\mu \rightarrow \infty$  we have the coherent Gaussian field.

Anyhow, the crucial point for our purposes is that for GSM fields one can assign a complex parameter  $Q$  (Simon et al., 1984, 1985, 1988; Simon and Mukunda, 1993b; Dragoman, 1996; Başkal and Kim, 2002)

$$Q = \frac{1}{R} + i \frac{1}{k\sigma_I \delta}, \quad (134)$$

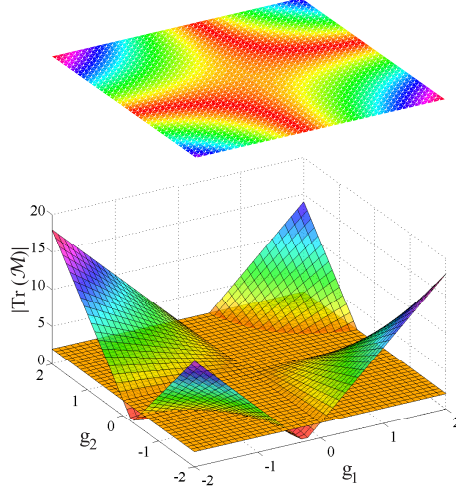


Figure 21: Plot of  $|\text{Tr}(\mathcal{M})|$  in terms of the parameters  $g_1$  and  $g_2$  of the optical resonator. The plane  $|\text{Tr}(\mathcal{M})| = 2$  is also shown. The density plot of the three-dimensional figure appears at the top.

where

$$\frac{1}{\delta} = \sqrt{\frac{1}{\sigma_\mu^2} + \frac{1}{4\sigma_I^2}}, \quad (135)$$

and  $R$  is the wave front curvature radius. This parameter fully characterizes the beam and satisfies the Kogelnik *abcd* law; namely, after propagation through a first-order optical system described by the matrix  $\mathcal{M}$  as in (64), the parameter  $Q$  changes to  $Q'$  via

$$Q' = \Phi[\mathcal{M}, Q] = \frac{dQ + c}{bQ + a}. \quad (136)$$

On account of  $\text{Im } Q > 0$  by the definition (134), one immediately checks that  $\text{Im } Q' > 0$  and we can thus view the action of the system as a bilinear transformation on the upper complex half-plane. When we use the metric  $ds = |dQ|/\text{Im } Q$  to measure distances, what we get again is the standard model of the hyperbolic plane  $\mathbb{H}$  (Stahl, 1993).

The whole real axis, which is the boundary of  $\mathbb{H}$ , is also invariant under (136) and represents wave fields with unlimited transverse irradiance (contrary to the notion of a beam). On the other hand, for the points in the imaginary axis we have an infinite wave front radius, which defines the corresponding beam waists. The origin renders a plane wave.

The geometrical scenario presented before allows one to describe the evolution of a GSM beam by means of the associated orbits. Let us go back to the example of the optical cavity treated in section 3.3. The associated transfer matrix  $\mathcal{M}$  fulfills

$$\text{Tr } \mathcal{M} = 2(2g_1g_2 - 1). \quad (137)$$

Since the trace determines the fixed point and the orbits of the system, the  $g$  parameters establish uniquely the geometrical action of the cavity. To illustrate this point, in figure 21 we have plotted the value of  $|\text{Tr}(\mathcal{M})|$  in terms of  $g_1$  and  $g_2$ . The plane  $|\text{Tr}(\mathcal{M})| = 2$ , which delimits the boundary

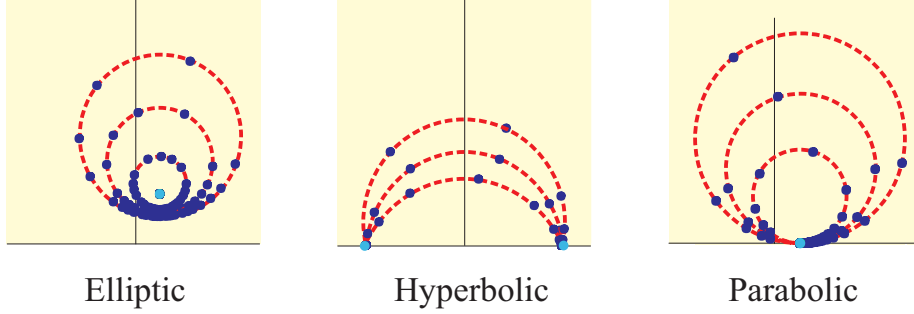


Figure 22: Successive iterates in the half plane  $\mathbb{H}$  for typical elliptic, hyperbolic, and parabolic actions. For hyperbolic and parabolic actions, the iterates tend to the real axis. The fixed points are marked in cyan.

between elliptic and hyperbolic action, is also shown. At the top of the figure, a density plot is presented, with the characteristic hyperbolic contours (Kogelnik and Li, 1966).

Assume now that the light bounces  $N$  times through this system. The overall transfer matrix is  $\mathcal{M}^N$  and the transformed beam is represented by

$$Q_N = \Phi[\mathcal{M}, Q_{N-1}] = \Phi[\mathcal{M}^N, Q_0], \quad (138)$$

where  $Q_0$  is the initial point.

Note that all the  $Q_N$  lie in the orbit associated to  $Q_0$  by the single round trip, which is determined by its fixed points. By varying the parameters  $g$  of the cavity we can choose to work in the elliptic, the hyperbolic, or the parabolic case (Başkal and Kim, 2002).

In figure 22 we have plotted the sequence of successive iterates for different kind of ray-transfer matrices, according to our previous classification. In the elliptic case, it is clear that the points  $Q_N$  revolve in the orbit centered at the fixed point and the system never reaches the real axis. On the contrary, for the hyperbolic and parabolic cases the iterates converge to one of the fixed points on the real axis, although with different laws (Barriuso et al., 2005a).

The iterates of hyperbolic and parabolic actions produce solutions fully unlimited, which are incompatible with our ideas of a beam. The only beam solutions are thus generated by elliptic actions and, according with equation (137), the stability criterion is

$$0 \leq |2g_1g_2 - 1| = |\cos(\phi/2)| \leq 1, \quad (139)$$

where  $\phi$  is the parameter in the canonical form  $\hat{\mathcal{K}}$  in equation (84). Such a condition is usually worked out in terms of algebraic arguments using ray-transfer matrices (Siegman, 1986).

#### 6.4. Quasiperiodic sequences

The most relevant property of periodic systems is the possibility of generating bandgaps for wave propagation. Spatial periodicity, however, is not necessarily a requirement for that: the presence of large bandgaps has been reported in aperiodic structures. Moreover, they share distinctive physical properties with both periodic (e.g., the formation of gaps) and disordered random media (e. g., the presence of highly localized states characterized by high-field enhancement and anomalous transport properties).

In few words, aperiodic structures are made up of two (or more) incomplete periods stacked together to form an overall system that is neither fully periodic nor random, but somewhere in

between (Maciá, 2009). These structures can be roughly sorted into two classes, those that are quasiperiodic and those that are not. The former present a discrete Fourier spectrum characterized by self-similar Bragg peaks (quite reminiscent of periodicity), whereas the latter usually exhibit complex diffraction spectra with singular scattering peaks, and multifractal scaling properties.

From a mathematical viewpoint quasiperiodic functions belong to the class of almost periodic functions (Bohr, 1951). These functions can be uniformly approximated by Fourier series containing a countable infinity of pairwise incommensurate frequencies. When the set of frequencies required can be generated from a finite-dimensional basis, the resulting function is referred to as a quasiperiodic one. The simplest example of a quasiperiodic function is

$$V(x) = \cos x + \cos(\lambda x), \quad (140)$$

where  $\lambda$  is an irrational number.

Additionally, quasiperiodic structures lack translational invariance but possess a high degree of rotational symmetry, while the not quasiperiodic lack both translational and rotational symmetry but display remarkable self-similarity (scale invariance symmetry) in their structural and spectral features (Maciá, 2006).

The interest in these sequences was originally fueled by the theoretical predictions that they should manifest peculiar electron and phonon critical states (Ostlund and Pandit, 1984; Kohmoto et al., 1987), associated with highly fragmented fractal energy spectra (Kohmoto et al., 1983; Luck, 1989; Sütö, 1989; Bellissard et al., 1989; Oh and Lee, 1993; Chakrabarti et al., 1995; Liu, 1997; Monsoriu et al., 2006). On the other hand, the practical fabrication of Fibonacci (Merlin et al., 1985) and Thue-Morse (Merlin et al., 1987) superlattices triggered a number of experimental achievements that have provided new insights into the capabilities of quasiperiodic structures (Zárate and Velasco, 2001; Velasco and García-Moliner, 2003; Albuquerque and Cottam, 2003). In particular, possible optical applications have deserved major attention and some intriguing properties have been demonstrated (Tamura and Nori, 1989; Avishai and Berend, 1990; Kolář et al., 1991; Hattori et al., 1994; Vasconcelos and Albuquerque, 1999; Hollingworth et al., 2001; Lusk et al., 2001; Barriuso et al., 2005b; Mugassabi and Vourdas, 2009). Underlying all these theoretical and experimental efforts a crucial fundamental question remains concerning whether quasiperiodic devices would achieve better performance than usual periodic ones for some specific applications (Maciá, 2001; Barriuso et al., 2003a).

A simple understanding of a well ordered but aperiodic arrangement of numbers can be grasped by thinking of the Fibonacci numbers sequence  $F_n = \{1, 1, 2, 3, 5, 8, 13, 21, \dots\}$ . The terms in this sequence are generated from the recursive equation  $F_{n+1} = F_n + F_{n-1}$ , starting with  $F_0 = 1$  and  $F_1 = 1$ . Hence, each number in the sequence is just the sum of the preceding two. The sequence is then perfectly ordered, but the rule used to generate it has nothing to do with periodicity. The symbolical analog of the Fibonacci sequence, constructed using two types of building blocks, say  $A$  and  $B$ , can be obtained from the substitution rule  $A \mapsto AB$  and  $B \mapsto A$ , whose successive application generates the sequence of letters  $A, AB, ABA, ABAAB, ABAABABA, \dots$  and so on. In this way, we get a perfectly ordered word which is not periodic at all.

The standard method of constructing aperiodic structures is thus through a substitution rule operating on a finite alphabet  $\{A, B, \dots\}$ , which consists of certain number of letters. In actual realizations each letter will correspond to a different type of building block in the structure. In particular, the substitutional sequences that act upon a two-letter alphabet  $\{A, B\}$  are especially

Table 1: List of the substitution rules determining the sequences usually considered in the study of self-similar aperiodic systems.

Sequence	Alphabet	Substitution rule
Fibonacci	$\{A, B\}$	$\sigma_1 = AB, \sigma_2 = A$
Thue-Morse	$\{A, B\}$	$\sigma_1 = AB, \sigma_2 = BA$
Period doubling	$\{A, B\}$	$\sigma_1 = AB, \sigma_2 = AA$
Rudin-Shapiro	$\{A, B, C, D\}$	$\sigma_1 = AC, \sigma_2 = DC, \sigma_3 = AB, \sigma_4 = DB$
Circular	$\{A, B, C\}$	$\sigma_1 = CAC, \sigma_2 = ACCAC, \sigma_3 = ABCAC$

important: in this case the algorithm reduces to

$$A \mapsto \sigma_1(A, B), \quad B \mapsto \sigma_2(A, B), \quad (141)$$

where  $\sigma_1$  and  $\sigma_2$  can be any string of  $A$  and  $B$ . In table 1 we list some representatives among the plethora of aperiodic structures grown during the last two decades.

To each rule we can associate a substitution matrix  $T$ , whose columns give the number the letters  $A$  and  $B$  which occur in the substitutions  $\sigma_1$  and  $\sigma_2$

$$T = \begin{pmatrix} n_A[\sigma_1(A, B)] & n_A[\sigma_2(A, B)] \\ n_B[\sigma_1(A, B)] & n_B[\sigma_2(A, B)] \end{pmatrix}. \quad (142)$$

This matrix does not depend on the precise form of the substitutions (the order of the letters), only on the number of letters  $A$  or  $B$ .

The eigenvalues of the substitution matrix  $T$  contain a lot of information. In fact, according to a theorem by Bombieri and Taylor (1986), if the spectrum of  $T$  contains a Pisot number, the structure is quasiperiodic; otherwise it is not. A Pisot number is a positive algebraic number (i.e., a number that is a solution of an algebraic equation) greater than one, all of whose conjugate elements (the other solutions of the algebraic equation) have modulus less than unity (Bertin et al., 1992; Godrèche and Luck, 1992). For example, let us consider the sequence  $\sigma_1 = AAAB$ ,  $\sigma_2 = BBA$ , whose characteristic matrix is:

$$T = \begin{pmatrix} 3 & 1 \\ 1 & 2 \end{pmatrix}. \quad (143)$$

The eigenvalues are  $\lambda_1 = (5 + \sqrt{5})/2$  and  $\lambda_2 = (5 - \sqrt{5})/2$ . Since  $\lambda_1 > \lambda_2 > 1$ , the sequence does posses the Pisot property. In Table 2 we give a sketch of the properties of the substitutional sequences considered thus far.

The sequences can be also characterized by the nature of their Fourier spectrum (Severin and Riklund, 1989). The Fourier spectrum corresponding to a perfect infinite periodic system contains delta functions centered in wave numbers associated to the reciprocal lattice (this is the origin of the Bragg peaks). On the contrary, a disordered structure has a very flat spectrum. Aperiodic heterostructures following a deterministic sequence display characteristic spectral properties absent in either of these extreme cases.

For a specific sequence of length  $N$ , the discrete Fourier transform is

$$W_N(k) = \frac{1}{\sqrt{N}} \sum_{j=1}^{N-1} w(j) \exp\left(\frac{-2\pi i k j}{N}\right), \quad (144)$$



Table 2: Substitution matrices and related eigenvalues for the sequences listed in Table 1.

Sequence	Substitution matrix	Eigenvalues
Fibonacci	$\begin{pmatrix} 1 & 1 \\ 1 & 0 \end{pmatrix}$	$\lambda_1 = (1 + \sqrt{5})/2, \lambda_2 = (1 - \sqrt{5})/2$
Thue-Morse	$\begin{pmatrix} 1 & 1 \\ 1 & 1 \end{pmatrix}$	$\lambda_1 = 2, \lambda_2 = 0$
Period doubling	$\begin{pmatrix} 1 & 1 \\ 2 & 0 \end{pmatrix}$	$\lambda_1 = 2, \lambda_2 = -1$
Rudin-Shapiro	$\begin{pmatrix} 1 & 0 & 1 & 0 \\ 0 & 0 & 1 & 1 \\ 1 & 1 & 0 & 0 \\ 0 & 1 & 0 & 1 \end{pmatrix}$	$\lambda_1 = 0, \lambda_2 = 2, \lambda_3 = \sqrt{2}, \lambda_4 = -\sqrt{2}$
Circular	$\begin{pmatrix} 1 & 0 & 2 \\ 2 & 0 & 3 \\ 2 & 1 & 2 \end{pmatrix}$	$\lambda_1 = -1, \lambda_2 = 2 + \sqrt{5}, \lambda_3 = 2 - \sqrt{5}$

where  $w(j)$  is a numerical sequence obtained by assigning to each letter of the alphabet a fixed amplitude. This assignment is otherwise arbitrary and does not change any conclusion. In consequence, one could, e.g., use  $A \mapsto -1$  and  $B \mapsto 1$ . The structure factor (or power spectrum) is (Cheng and Savit, 1990)

$$S_N(k) = |W_N(k)|^2. \quad (145)$$

From a rigorous viewpoint, the only well-established concept attached to the Fourier spectrum is its spectral measure. If we define

$$d\nu_N(k) = S_N(k)dk, \quad (146)$$

we will be concerned with the nature of the limit

$$d\nu(k) = \lim_{N \rightarrow \infty} d\nu_N(k), \quad (147)$$

which corresponds to an infinite structure and a continuous variable  $k$ . Just as any positive measure, (147) has a unique decomposition (Reed and Simon, 1980)

$$d\nu(k) = d\nu_{\text{pp}}(k) + d\nu_{\text{ac}}(k) + d\nu_{\text{sc}}(k) \quad (148)$$

into its pure point, absolutely continuous and singular continuous parts.

The pure point part refers to the presence of Bragg peaks; the absolute continuous part is a differentiable function (diffuse scattering), while the singular continuous part it is neither continuous nor does it have Bragg peaks. It shows broad peaks, which are never isolated and, with increasing resolution, split again into further broad.

The Fibonacci sequence has a pure point spectrum; the Thue-Morse sequence has a singular continuous Fourier spectrum, while the Rudin-Shapiro sequence shows an absolute continuous one. For a very detailed and up-to-date discussion of these issues, the reader is referred to comprehensive book by Maciá (2009).

### 6.5. Hyperbolic tilings

The rich properties of these aperiodic structures suggest the utility of studying of systems based on more general sequences (Spinadel, 1999). Periodicity is intimately connected with tessellations, i.e., tilings by identical replicas of a unit cell (or fundamental domain) that fill the plane with no overlaps and no gaps. Of special interest is the case when the primitive cell is a regular polygon with a finite area (Zieschang et al., 1980). In the Euclidean plane, the associated regular tessellation is generically noted  $\{p, q\}$ , where  $p$  is the number of polygon edges and  $q$  is the number of polygons that meet at a vertex. Geometrical constraints limit the possible regular tilings  $\{p, q\}$  to those verifying

$$(p-2)(q-2) = 4. \quad (149)$$

This includes the classical tilings  $\{4, 4\}$  (tiling by squares) and  $\{6, 3\}$  (tiling by hexagons), plus a third one, the tiling  $\{3, 6\}$  by triangles (which is dual to the  $\{6, 3\}$ ).

On the contrary, in the hyperbolic disk regular tilings exist provided  $(p-2)(q-2) > 4$ , which now leads to an infinite number of possibilities (Magnus, 1974). The fundamental polygons are connected to the discrete subgroups of isometries (or congruent mappings); they are Fuchsian groups (Ford, 1972) and play for the hyperbolic geometry a role similar to that of crystallographic groups for the Euclidean geometry (Beardon, 1983).

A tessellation of the hyperbolic plane by regular polygons has a symmetry group that is generated by reflections in geodesics, which are inversions across circles in the unit disc. These geodesics correspond to edges or axes of symmetry of the polygons. Therefore, to construct a tessellation of the unit disk one just has to built one tile and to duplicate it by using reflections in the edges.

To go straight to the point let us consider the following parabolic transformations

$$A = \begin{pmatrix} 1-i & 1 \\ 1 & 1+i \end{pmatrix}, \quad B = \begin{pmatrix} 1+i & 1 \\ 1 & 1-i \end{pmatrix}, \quad (150)$$

with fixed points  $+i$  and  $-i$ , respectively. A possible implementation of these matrices (and their inverses) in terms of two commonly employed materials can be found in Barriuso et al. (2009). In figure 23, we have plotted the tessellation obtained by transforming the fundamental square with the Fuchsian group generated by the powers of  $\{A, B\}$  (and the inverses).

To give an explicit construction rule for the admissible words, we proceed as follows. First, we arbitrarily choose a side of the fundamental square and assign to it the value 0. Then the other three sides are numbered clockwise as 1, 2 and 3. It is easy to convince oneself that this assignment fixes once and for all the numbering for the sides of all the other squares in the tessellation. However, these squares can be distinguished by their orientation (as seen from the corresponding center): the clockwise oriented ones are filled in red, while the counterclockwise ones are filled in yellow. In short, we have determined a fundamental coloring of the tessellation (Grünbaum and Shepard, 1987).

To derive a center  $z_{n+1}$  from a previous one  $z_n$ , one looks first at the corresponding color jump. Next, the matrix that takes  $z_n$  into  $z_{n+1}$  depends on the numbering of the side (0, 1, 2, or 3) one must cross, and appears in the column labeled  $T$  in table 3. The next generation is obtained in much the same way, except for the fact that  $A_n$  and  $B_n$  must be replaced by  $A_{n+1}$  and  $B_{n+1}$ , respectively, as indicated in the table. In creating recursively any word, the origin is denoted as  $z_0$  and the matrices  $A_0$  and  $B_0$  coincide with  $A$  and  $B$ . One can then construct any word step by

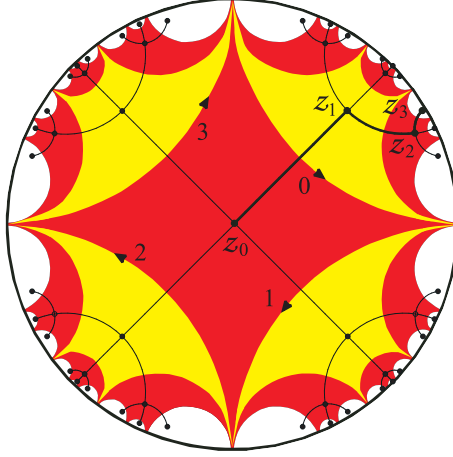


Figure 23: Tessellation of the unit disk with the matrices (150). The marked points are the centers of the squares. All of them are the transformed of the origin by a matrix that have as reflection coefficient the complex number that links the origin with the center of the square.

Table 3: Explicit rules to obtain the center  $z_{n+1}$  from  $z_n$  in the tiling by hyperbolic squares. We have indicated the corresponding transformations, which depend on the color jump and the sides crossed by going from  $z_n$  to  $z_{n+1}$ .

Side	$T$	red $\rightarrow$ yellow		$T$	yellow $\rightarrow$ red	
		$A_{n+1}$	$B_{n+1}$		$A_{n+1}$	$B_{n+1}$
0	$A_n$	$B_n$	$A_n B_n A_n^{-1}$	$A_n^{-1}$	$A_n$	$A_n^{-1} B_n A_n$
1	$B_n$	$B_n A_n B_n^{-1}$	$B_n$	$B_n^{-1}$	$B_n^{-1} A_n B_n$	$B_n$
2	$B_n^{-1}$	$B_n^{-1} A_n B_n$	$B_n$	$B_n$	$B_n A_n B_n^{-1}$	$B_n$
3	$A_n^{-1}$	$A_n$	$A_n^{-1} B_n A_n$	$A_n$	$A_n$	$A_n B_n A_n^{-1}$

step. For example, the word that transforms  $z_0$  into  $z_6$  in the zig-zag path sketched in figure 23 results:

$$\begin{aligned}
 z_0 \rightarrow z_1 & : A, \\
 z_1 \rightarrow z_2 & : AB^{-1}A^{-1}, \\
 z_2 \rightarrow z_3 & : AB^{-1}A^{-1}, \\
 z_3 \rightarrow z_4 & : AB^{-1}B^{-1}ABBA^{-1}, \\
 z_4 \rightarrow z_5 & : AB^{-1}B^{-1}ABBA^{-1}, \\
 z_5 \rightarrow z_6 & : AB^{-1}B^{-1}AAB^{-1}A^{-1}A^{-1}BBA^{-1}.
 \end{aligned} \tag{151}$$

The characteristic matrices of these substitution rules are

$$T_{\text{odd}} = \begin{pmatrix} 1 & 0 & 1 & 1 \\ 2 & 1 & 3 & 1 \\ 1 & 1 & 1 & 0 \\ 3 & 1 & 2 & 1 \end{pmatrix}, \quad T_{\text{even}} = \begin{pmatrix} 1 & 0 & 0 & 0 \\ 0 & 1 & 0 & 0 \\ 0 & 0 & 1 & 0 \\ 0 & 0 & 0 & 1 \end{pmatrix} \tag{152}$$

with eigenvalues  $2 + \sqrt{5}$ ,  $2 - \sqrt{5}$ , 1 and  $-1$  for  $T_{\text{odd}}$  and 1 for  $T_{\text{even}}$  (that produces a trivial effect and will no be taken into account). Since one of the eigenvalues is greater than 1 and the others

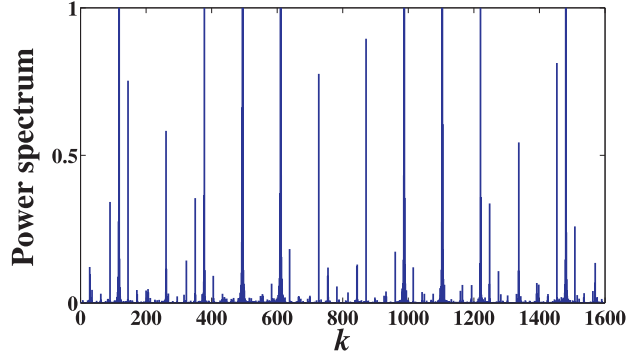


Figure 24: Normalized power spectrum for a word in the zig-zag path shown in figure 23 but with 1600 letters.

have an absolute value less than or equal to unity (with at least one of modulus 1), the substitution possesses the Salem property (Salem, 1963), property weaker than the Pisot property.

In figure 24 we have plotted the structure factor of this sequence for a word of 1600 letters that starts at the origin. Previously, we assigned to each letter in the alphabet the quartic roots of the identity, namely  $A \mapsto i$ ,  $B \mapsto +1$ ,  $A^{-1} \mapsto -i$ ,  $B^{-1} \mapsto -1$ . The gross features of the spectrum are seen to be humps separated by almost empty regions. Inside these humps, there is a blurred structure built up of packed delta-spikes. The dominant peaks tend to be isolated and larger.

To describe the continuous part of the measure in an analytical way seems to be a hard task. Still we can introduce the integrals (Aubry et al., 1987; Godrèche and Luck, 1990)

$$\mathcal{I}_N = \int_0^{k_{\max}} \sqrt{S_N(k)} dk, \quad (153)$$

where  $k_{\max}$  is some arbitrary spectral cutoff. The nature of the limit measure is partly coded in the behavior of these quantities for large  $N$ . In fact, for an absolutely continuous measure they tend to be constant, while they scale as  $\mathcal{I}_N \sim N^{-1/2}$  for a pure point measure (Godrèche and Luck, 1992). A somehow intermediate behavior can be expected for the singular continuous case. For our system, we have evaluated numerically (153), finding the law

$$\mathcal{I}_N \sim N^{-\gamma}, \quad \gamma = 0.36 \pm 0.02. \quad (154)$$

This rules out the existence of an absolutely continuous component and suggests that only a singular spectrum is present. This exponent can also be related to the theory of multifractals: if the measure  $d\nu(k)$  has a generalized dimension function  $D_k$ , then  $\gamma$  should be linearly related to  $D_k$  (Hentschel and Procaccia, 1983).

## 7. Concluding remarks

This review is concerned with the transfer matrix, a powerful tool that relies only on the linearity of a system with two input and two output channels. Therefore, it is not surprising the variety of domains in which this object has been successfully employed.

Instead of embarking in a detailed description of a particular model, our thread has been to put geometry to work. This provides a useful and, at the same time, simple language in which numerous physical ideas may be clearly formulated and effectively treated.

In a first step, we have transplanted the transfer matrix into space-time phenomena. This gateway works in both directions: here, it has allowed us to establish a relativistic presentation of the transfer matrix, but specific models can be also used as an instrument for visualizing special relativity. This is more than an academic curiosity: in fact, some intricate relativistic effects, such as, e.g., the Wigner angle, can be measured (and not merely inferred) by optical setups.

By resorting to elementary notions of hyperbolic geometry, we have interpreted in a natural way the action of the transfer matrix as a mapping on the unit disk and on the upper half-plane. The trace turns out to classify and characterize the basic geometrical actions, which has physical relevance. In fact, in this arena, nontrivial phenomena can be understood in terms of analogues of vectors in Euclidean geometry.

We have applied this perspective to periodic systems, explaining the existence of bandgaps in appealing terms. In addition, we have presented schemes to generate quasiperiodic sequences based on tessellations of the unit disc.

Nothing of the material presented here is applicable *per se*, but everything can be relevant for researchers in other fields. This is the beauty of the approach. To our mind, the manuscript is better than ever. May each reader benefit and enjoy!

## Acknowledgments

Our efforts towards understanding the problems posed in this paper were fueled in part, and were made much more interesting, by the interaction with a number of colleagues and friends. We warmly thank Gunnar Björk, Luis Joaquín Boya, Antonio F. Costa, Angel Felipe, Alberto Galindo, Hubert de Guise, Andrei Klimov, Gerd Leuchs, Carlos López Lacasta, Enrique Maciá, José María Montesinos, Mariano Santander, and Teresa Yonte.

Financial support from the Spanish Research Agency (Grants FIS2005-06714, FIS2008-04356, FIS2011-26786) and the UCM-BCSH program (Grant GR-920992) is gratefully acknowledged.

## References

- Abe, S., Sheridan, J. T., 1994. Optical operations on wave functions as the Abelian subgroups of the special affine Fourier transformation. *Opt. Lett.* 19, 1801–1803.
- Abelès, F., 1948. Sur la propagation des ondes électromagnétiques dans les milieux stratifiés. *Ann. Phys. (Paris)* 3, 504–520.
- Abramowitz, M., Stegun, I. A. (Eds.), 1996. *Handbook of Mathematical Functions*. Dover, New York.
- Ahn, D., Chuang, S. L., 1986. Variational calculations of subbands in a quantum well with uniform electric field: Gram-Schmidt orthogonalization approach. *Appl. Phys. Lett.* 49, 1450–1452.
- Aktosun, T., 1992. A factorization of the scattering matrix for the Schrödinger equation and for the wave equation in one dimension. *J. Math. Phys.* 33, 3865–3869.
- Aktosun, T., Klaus, M., van der Mee, C., 1996. Factorization of scattering matrices due to partitioning of potentials in one-dimensional Schrödinger-type equations. *J. Math. Phys.* 37, 5897–5915.
- Albeverio, S., Gesztesy, F., Hoegh-Krohn, R., Holden, H., 2004. *Solvable Models in Quantum Mechanics*. AMS, Providence.
- Albuquerque, E. L., Cottam, M. G., 2003. Theory of elementary excitations in quasiperiodic structures. *Phys. Rep.* 376, 225–337.

- Ambrosini, D., Bagini, V., Gori, F., Santarsiero, M., 1994. Twisted Gaussian Schell-model beams: A superposition model. *J. Mod. Opt.* 41, 1391–1399.
- Anderson, J. W., 1999. *Hyperbolic Geometry*. Springer, New York.
- Ando, T., Taniyama, H., Ohtani, N., Nakayama, M., Hosoda, M., 2003. Self-consistent calculation of subband occupation and electron-hole plasma effects: Variational approach to quantum well states with Hartree and exchange-correlation interactions. *J. Appl. Phys.* 94, 4489–4501.
- Aravind, P. K., 1997. The Wigner angle as an anholonomy in rapidity space. *Am. J. Phys.* 65, 634–636.
- Arsenault, H. H., Macukow, B., 1983. Factorization of the transfer matrix for symmetrical optical systems. *J. Opt. Soc. Am.* 73, 1350–1359.
- Ashcroft, N. W., Mermin, N. D., 1976. *Solid State Physics*. Saunders, Philadelphia.
- Aubry, S., Godrèche, C., Luck, J. M., 1987. A structure intermediate between quasi-periodic and random. *Europhys. Lett.* 4, 639–643.
- Avishai, Y., Berend, D., 1990. Transmission through a one-dimensional Fibonacci sequence of delta-function potentials. *Phys. Rev. B* 41, 5492–5499.
- Azzam, R., Bashara, N., 1987. *Ellipsometry and Polarized Light*. North-Holland, Amsterdam.
- Ballentine, L. F., 1998. *Quantum Mechanics*. World Scientific, Singapore.
- Barlette, V. E., Leite, M. M., Adhikar, S. K., 2001. Integral equations of scattering in one dimension. *Am. J. Phys.* 69, 1010–1013.
- Barlette, V. E., Leite, M. M., Adhikari, S. K., 2000. Quantum scattering in one dimension. *Eur. J. Phys.* 21, 435–440.
- Barra, F., Gaspard, P., 1999. Scattering in periodic systems: From resonances to band structure. *J. Phys. A* 32, 3357–3375.
- Barriuso, A. G., Monzón, J. J., Sánchez-Soto, L. L., 2003a. General unit-disk representation for periodic multilayers. *Opt. Lett.* 28, 1501–1503.
- Barriuso, A. G., Monzón, J. J., Sánchez-Soto, L. L., Cariñena, J. F., 2003b. Hyperbolic reflections as fundamental building blocks for multilayer optics. *J. Opt. Soc. Am. A* 20, 1812–1817.
- Barriuso, A. G., Monzón, J. J., Sánchez-Soto, L. L., Cariñena, J. F., 2004. Vectorlike representation of multilayers. *J. Opt. Soc. Am. A* 21, 2386–2391.
- Barriuso, A. G., Monzón, J. J., Sánchez-Soto, L. L., Cariñena, J. F., 2005a. Geometrical aspects of first-order optical systems. *J. Opt. A* 7, 451–456.
- Barriuso, A. G., Monzón, J. J., Sánchez-Soto, L. L., Costa, A. F., 2009. Escher-like quasiperiodic heterostructures. *J. Phys. A* 42, 192002.
- Barriuso, A. G., Monzón, J. J., Sánchez-Soto, L. L., Felipe, A., 2005b. Comparing omnidirectional reflection from periodic and quasiperiodic one-dimensional photonic crystals. *Opt. Express* 13, 3913–3920.
- Barut, A. O., 1980. *Electrodynamics and Classical Theory of Fields and Particles*. Dover, New York.
- Barut, A. O., Rączka, R., 1977. *Theory of Group Representations and Applications*. PWN, Varsovia.
- Başkal, S., Georgieva, E., Kim, Y. S., Noz, M. E., 2004. Lorentz group in classical ray optics. *J. Opt. B* 6, 4455–4472.
- Başkal, S., Kim, Y., 2002. Wigner rotations in laser cavities. *Phys. Rev. E* 66, 026604.
- Bastard, G., 1981. Superlattice band structure in the envelope-function approximation. *Phys. Rev. B* 24, 5693–5697.
- Bastard, G., Méndez, E. E., Chang, L. L., Esaki, L., 1983. Variational calculations on a quantum well in an electric field. *Phys. Rev. B* 28, 3241–3245.
- Beardon, A. F., 1983. *The Geometry of Discrete Groups*. Springer, New York.
- Bellissard, J., Iochum, B., Scoppola, E., Testard, D., 1989. Spectral properties of one dimensional quasi-crystals. *Comm. Math. Phys.* 125, 527–543.
- Ben-Menahem, A., 1985. Wigner's rotation revisited. *Am. J. Phys.* 53, 62–66.
- Bendickson, J. M., Dowling, J. P., Scalora, M., 1996. Analytic expressions for the electromagnetic mode density in finite, one-dimensional, photonic band-gap structures. *Phys. Rev. E* 53, 4107–4121.
- Bertin, M. J., Decomps-Guilloux, A., Grandet-Hugot, M., Pathiaux-Delefosse, M., Schreiber, J. P., 1992. *Pisot and Salem Numbers*. Birkhäuser, Berlin.
- Biedenharn, L. C., Louck, J. D., 1981. *Angular Momentum in Quantum Physics*. Addison, Reading, MA.
- Bohm, D., 1989. *Quantum Theory*. Dover, New York.
- Bohr, H., 1951. *Almost Periodic Functions*. Chelsea, New York.
- Bombieri, E., Taylor, J. E., 1986. Which distributions of matter diffract? an initial investigation. *J. Phys. Colloq.* 47 (C3), 19–28.
- Boonserm, P., Visser, M., 2009. Transmission probabilities and the Miller-Good transformation. *J. Phys. A* 42, 045301.
- Boonserm, P., Visser, M., 2010a. Analytic bounds on transmission probabilities. *Ann. Phys.* 325, 1328–1339.
- Boonserm, P., Visser, M., 2010b. One dimensional scattering problems: A pedagogical presentation of the relationship between reflection and transmission amplitudes. *Thai J. Math.* 8, 83–97.
- Born, M., Wolf, E., 1999. *Principles of Optics*. Cambridge University Press, Cambridge.
- Boya, L. J., 2008. Quantum-mechanical scattering in one dimension. *Riv. Nuovo Cimento* 31, 75–139.
- Brekovskikh, L. M., 1960. *Waves in Layered Media*. Academic, New York.

- Burt, M. G., 1992. The justification for applying the effective-mass approximation to microstructures. *J. Phys.: Condens. Matter* 4, 6651–6690.
- Busch, K., von Freymann, G., Linden, S., Mingaleev, S. F., Tkeshelashvili, L., Wegener, M., 2007. Periodic nanostructures for photonics. *Phys. Rep.* 444, 101–202.
- Cai, W., Shalaev, V., 2009. *Optical Metamaterials: Fundamentals and Applications*. Springer, Berlin.
- Cao, Z., Liu, Q., Shen, Q., Dou, X., Chen, Y., Ozaki, Y., 2001. Quantization scheme for arbitrary one-dimensional potential wells. *Phys. Rev. A* 63, 054103.
- Cattapan, G., Maglione, E., 2003. Coupled-channel integral equations for quasi one-dimensional systems. *Am. J. Phys.* 71, 903–911.
- Chakrabarti, A., Karmakar, S. N., Moitra, R. K., 1995. Role of a new type of correlated disorder in extended electronic states in the Thue-Morse lattice. *Phys. Rev. Lett.* 74, 1403–1406.
- Chebotarev, L. V., 1995. Transmission spectra for one-dimensional potentials in the semiclassical approximation. *Phys. Rev. A* 52, 107–124.
- Chebotarev, L. V., 1997. The postclassical approximation in quantum tunnelling. *Eur. J. Phys.* 18, 188–193.
- Chebotarev, L. V., Tchibotareva, A., 1996. Flat resonances in one-dimensional quantum scattering. *J. Phys. A* 29, 7259–7277.
- Chen, J.-L., Ge, M.-L., 1998. On the Wigner angle and its relation with the defect of a triangle in hyperbolic geometry. *J. Geom. Phys.* 25, 341–345.
- Cheng, Z., Savit, R., 1990. Structure factor of substitutional sequences. *J. Stat. Phys.* 60, 383–393.
- Chuprikov, N. L., 1996. Tunneling in a one-dimensional system of  $N$  identical potential barriers. *Semiconductors* 30, 246–251.
- Cohen-Tannoudji, C., Diu, B., Laloë, F., 1977. *Quantum Mechanics*. Vol. 1. Wiley, New York.
- Corzine, S. W., Yan, R. H., Coldren, L. A., 1991. A tanh-substitution technique for the analysis of abrupt and graded interface multilayer dielectric stacks. *IEEE J. Quantum Electron.* 27, 2086–2090.
- Coxeter, H. S. M., 1968. *Non-Euclidean Geometry*. University of Toronto Press, Toronto.
- Coxeter, H. S. M., 1969. *Introduction to Geometry*. Wiley, New York.
- Crawford, F. S., 1968. *Waves*. Vol. 3 of Berkeley Physics Course. McGraw, New York.
- Cvetič, C., Pičman, L., 1981. Scattering states for a finite chain in one dimension. *J. Phys. A* 14, 379–382.
- Dragoman, D., 1996. The Wigner distribution function and the energy conservation of a light beam. *J. Mod. Opt.* 43, 1127–1133.
- Dragoman, D., Dragoman, M., 2007. Metamaterials for ballistic electrons. *J. Appl. Phys.* 101, 104316.
- Eberly, J. H., 1965. Quantum scattering theory in one dimension. *Am. J. Phys.* 33, 771–773.
- Erdős, P., Livioiti, E., Herndon, R. C., 1997. Wave transmission through lattices, superlattices and layered media. *J. Phys. D* 30, 338–345.
- Esaki, L., 1986. A birds-eye-view on the evolution of semiconductor superlattices and quantum wells. *IEEE J. Quantum Electron.* QE-22, 1611–1624.
- Felbacq, D., Guizal, B., Zolla, F., 1998. Wave propagation in one-dimensional photonic crystals. *Opt. Commun.* 152, 119–126.
- Foley, J., Zubairy, M. S., 1978. The directionality of Gaussian Schell-model beams. *Opt. Commun.* 26, 297–300.
- Ford, L. R., 1972. *Automorphic Functions*. Chelsea, New York.
- Formánek, J., 1976. On phase shift analysis of one-dimensional scattering. *Am. J. Phys.* 44, 778–779.
- Friberg, A. T., Sudol, R. J., 1982. Propagation parameters of Gaussian Schell-model beams. *Opt. Commun.* 41, 383–387.
- Friberg, A. T., Turunen, J., 1988. Imaging of Gaussian Schell-model sources. *J. Opt. Soc. Am. A* 5, 713–720.
- Galindo, A., Pascual, P., 1990. *Quantum Mechanics*. Vol. 1. Springer, Berlin.
- Gantmacher, F. R., 2000. *Matrix Theory*. Vol. 1 and 2. Chelsea, New York.
- García-Moliner, F., Velasco, V. R., 1992. *Theory of Single and Multiple Interfaces: The Method of Surface Green Function Matching*. World Scientific, Singapore.
- Gerrard, A., Burch, J. M., 1975. *Introduction to Matrix Methods in Optics*. Wiley, New York.
- Giust, R., Vigoureux, J. M., 2002. Hyperbolic representation of light propagation in a multilayer medium. *J. Opt. Soc. Am. A* 19, 378–384.
- Giust, R., Vigoureux, J. M., Lages, J., 2009. Generalized composition law from 2x2 matrices. *Am. J. Phys.* 77, 1068–1073.
- Gloge, D., Marcuse, D., 1969. Formal quantum theory of light rays. *J. Opt. Soc. Am.* 59, 1629–1631.
- Godrèche, C., Luck, J. M., 1990. Multifractal analysis in reciprocal space and the nature of the Fourier transform of self-similar structures. *J. Phys. A* 23, 3769–3797.
- Godrèche, C., Luck, J. M., 1992. Indexing the diffraction spectrum of a non-Pisot self-similar structure. *Phys. Rev. B* 45, 176–185.
- Goldberger, M. L., Watson, K. M., 1964. *Collision Theory*. Wiley, New York.
- Gori, F., 1983. Mode propagation of the field generated by Collett-Wolf Schell-model sources. *Opt. Commun.* 46, 149–

- Gori, F., Grella, R., 1984. Shape invariant propagation of polychromatic fields. *Opt. Commun.* 49, 173–177.
- Gould, S. H., 1995. *Variational Methods for Eigenvalue Problems*. Dover, New York.
- Griffiths, D. J., Steinke, C. A., 2001. Waves in locally periodic media. *Am. J. Phys.* 69, 137–154.
- Griffiths, D. J., Taussig, N. F., 1992. Scattering from a locally periodic potential. *Am. J. Phys.* 60, 883–888.
- Grossel, P., Depasse, F., Vigoureux, J. M., 2002. Reflection and transmission behaviour of a particle in a resonant tunnelling barrier. *J. Phys. A* 35, 9787–9800.
- Grossel, P., Vigoureux, J. M., Baïda, F., 1994. Nonlocal approach to scattering in a one-dimensional problem. *Phys. Rev. A* 50, 3627–3637.
- Grünbaum, B., Shepard, G. C., 1987. *Tilings and Patterns*. Freeman, New York.
- Guillemin, V., Sternberg, S., 1984. *Symplectic Techniques in Physics*. Cambridge University Press, Londres.
- Hamilton, J. D., 1996. Relativistic precession. *Am. J. Phys.* 64, 1197–1201.
- Hamilton, W. R., 1853. *Lectures on Quaternions*. Hodges & Smith, Dublin.
- Hattori, T., Tsurumachi, N., Kawato, S., Nakatsuka, H., 1994. Photonic dispersion relation in a one-dimensional quasicrystal. *Phys. Rev. B* 50, 4220–4223.
- Hauge, E. H., Stovne, J. A., 1989. Tunneling times: a critical review. *Rev. Mod. Phys.* 61, 917–936.
- Hayata, K., Koshiba, M., Nakamura, K., Shimizu, A., 1988. Eigenstate calculations of quantum well structures using finite elements. *Electron. Lett.* 24, 614–616.
- He, Y., Cao, Z., Shen, Q., 2005. Analytical formula of the transmission probabilities across arbitrary potential barriers. *J. Phys. A* 38, 5771–5780.
- Helgason, S., 1978. *Differential Geometry, Lie Groups and Symmetric Spaces*. Academic Press, New York.
- Hentschel, H. G. E., Procaccia, I., 1983. The infinite number of generalized dimensions of fractals and strange attractors. *Physica D* 8, 435–444.
- Hollingworth, J. M., Vourdas, A., Backhouse, N., 2001. Wave propagation in one-dimensional optical quasiperiodic systems. *Phys. Rev. E* 64, 036611.
- Hutem, A., Sricheewin, C., 2008. Ground-state energy eigenvalue calculation of the quantum mechanical well  $v(x) = \frac{1}{2}kx^2 + \lambda x^4$  via analytical transfer matrix method. *Eur. J. Phys.* 29, 577–588.
- Jackson, J. D., 1975. *Classical Electrodynamics*. Wiley, New York.
- James, P. B., 1970. Integral equation formulation of one-dimensional quantum mechanics. *Am. J. Phys.* 38, 1319–1323.
- Jaworski, W., Wardlaw, D. M., 1989. Sojourn time, sojourn time operators, and perturbation theory for one-dimensional scattering by a potential barrier. *Phys. Rev. A* 40, 6210–6218.
- Jirauschek, C., 2009. Accuracy of transfer matrix approaches for solving the effective mass Schrödinger equation. *IEEE J. Quantum Electron.* 45, 1059–1067.
- Joannopoulos, J. D., Meade, R. D., Winn, J. N., 1995. *Photonic Crystals*. Princeton University Press, Princeton.
- Jonsson, B., Eng, S. T., 1990. Solving the Schrödinger equation in arbitrary quantum-well potential profiles using the transfer matrix method. *IEEE J. Quantum Electron.* 26, 2025–2035.
- Jordan, T. F., 1988. Berry phases and unitary transformations. *J. Math. Phys.* 29, 2042–2052.
- Juárez, M., Santander, M., 1982. Turns for the Lorentz group. *J. Phys. A* 15, 3411–3424.
- Kalos, M. J., Whitlock, P. A., 2007. *Monte Carlo Methods*. Wiley, Manheim.
- Kalotas, T. M., Lee, A. R., 1991. One-dimensional quantum interference. *Eur. J. Phys.* 12, 275–282.
- Kamal, A. N., 1984. On the scattering theory in one dimension. *Am. J. Phys.* 52, 46–49.
- Kapeluszny, J., Kuczumow, T., Reich, S., 1999. The Denjoy-Wolff theorem in the open unit ball of a strictly convex Banach space. *Adv. Math.* 143, 111–123.
- Kauderer, M., 1994. *Symplectic Matrices: First Order Systems and Special Relativity*. World Scientific, Singapore.
- Kennett, B. L. N., 1983. *Seismic Wave Propagation in Stratified Media*. Cambridge University Press, Cambridge.
- Kerimov, G. A., Sezgin, M., 1998. On scattering systems related to the  $SO(2,1)$  group. *J. Phys. A* 31, 7901–7912.
- Khashan, M. A., 1979. A Fresnel formula for dielectric multilayer mirrors. *Optik* 54, 363–371.
- Khorasani, S., Adibi, A., 2003. Analytical solution of linear ordinary differential equations by differential transfer matrix method. *Electron. J. Diff. Equations* 79, 1–18.
- Khorasani, S., Mehrany, K., 2003. Differential transfer matrix method for solution of one-dimensional linear non-homogeneous optical structures. *J. Opt. Soc. Am. B* 20, 91–96.
- Kiang, D., 1974. Multiple scattering by a Dirac comb. *Am. J. Phys.* 42, 785–787.
- Kiers, K. A., van Dijk, W., 1996. Scattering in one dimension: The coupled Schrödinger equation, threshold behaviour and Levinson's theorem. *J. Math. Phys.* 37, 6033–6059.
- Kobayashi, K., 2006. Complementary media of electrons. *J. Phys.: Condens. Matter* 18, 3703–3720.
- Kogelnik, H., Li, T., 1966. Laser beams and resonators. *Appl. Opt.* 5, 1550–1567.
- Kohmoto, M., Kadanoff, L. P., Tang, C., 1983. Localization problem in one dimension: Mapping and escape. *Phys. Rev. Lett.* 50, 1870–1872.
- Kohmoto, M., Sutherland, B., Iguchi, K., 1987. Localization in optics: Quasiperiodic media. *Phys. Rev. Lett* 58, 2436–



- 2438.
- Kolář, M., Ali, M. K., Nori, F., 1991. Generalized Thue-Morse chains and their physical properties. *Phys. Rev. B* 43, 1034–1047.
- Kronig, R. L., Penney, W. G., 1931. Quantum mechanics of electrons in crystal lattices. *Proc. R. Soc. London Ser. A* 130, 499–513.
- Landau, L. D., Lifshitz, E. M., 2000. *The Classical Theory of Fields*. Vol. 2 of *Course of Theoretical Physics*. Pergamon, London.
- Landau, L. D., Lifshitz, E. M., 2001. *Electrodynamics of Continuous Media*. Vol. 8 of *Course of Theoretical Physics*. Pergamon, London.
- Lee, H.-W., Zysnarski, A., Kerr, P., 1989. One-dimensional scattering by a locally periodic potential. *Am. J. Phys.* 57, 729–734.
- Leibler, L., 1975. Effective-mass theory for carrier in graded mixed semiconductors. *Phys. Rev. B* 12, 4443–4451.
- Lekner, J., 1987. *Theory of Reflection*. Kluwer, Dordrecht.
- Lekner, J., 1994. Light in periodically stratified media. *J. Opt. Soc. Am. A* 11, 2892–2899.
- Lekner, J., 2000. Omnidirectional reflection by multilayer dielectric mirrors. *J. Opt. A* 2, 349–352.
- Levi, M., 1994. A 'bicycle wheel' proof of the Gauss-Bonnet theorem, dual cones and some mechanical manifestations of the Berry phase. *Expo. Math.* 12, 145–164.
- Lieb, E. H., Matthies, D. C., 1966. *Mathematical Physics in One Dimension*. Academic, New York.
- Liu, N.-H., 1997. Propagation of light waves in Thue-Morse dielectric multilayers. *Phys. Rev. B* 55, 3543–3547.
- Liu, Q. H., Cheng, C., Massoud, H. Z., 2004. The spectral grid method: A novel fast Schrödinger-equation solver for semiconductor nanodevice simulation. *IEEE T. Comput. Aid. D.* 23, 1200–1208.
- Liviotti, E., 1994. Transmission through one-dimensional periodic media. *Helv. Phys. Acta* 67, 767–768.
- Luck, J. M., 1989. Cantor spectra and scaling of gap widths in deterministic aperiodic systems. *Phys. Rev. B* 39, 5834–5849.
- Lusk, D., Abdulhalim, I., Placido, F., 2001. Omnidirectional reflection from Fibonacci quasi-periodic one-dimensional photonic crystal. *Opt. Commun.* 198, 273–279.
- Maciá, E., 2001. Exploiting quasiperiodic order in the design of optical devices. *Phys. Rev. B* 63, 205421.
- Maciá, E., 2006. The role of aperiodic order in science and technology. *Rep. Prog. Phys.* 69, 397–441.
- Maciá, E., 2009. *Aperiodic Structures in Condensed Matter: Fundamentals and Applications*. CRC Press, Boca Raton.
- Magnus, W., 1974. *Non-Euclidean Tessellations and their Groups*. Academic Press, New York.
- Malykin, G. B., 2006. Thomas precession: correct and incorrect solutions. *Phys. Usp.* 49, 837–853.
- Mandel, L., Wolf, E., 1995. *Optical Coherence and Quantum Optics*. Cambridge University Press, Cambridge.
- Marinov, M. S., Segev, B., 1996. Analytical properties of scattering amplitudes in one-dimensional quantum theory. *J. Phys. A* 29, 2839–2851.
- Martorell, J., Sprung, D. W. L., Morozov, G. V., 2004. Design of electron band pass filters for electrically biased finite superlattices. *Phys. Rev. B* 69, 115309.
- Mathews, P. M., Venkatesan, K., 1978. *A Textbook of Quantum Mechanics*. McGraw-Hill, New York.
- Merlin, R., Bajema, K., Clarke, R., Juang, F. Y., Bhattacharya, P. K., 1985. Quasiperiodic GaAs-AlAs heterostructures. *Phys. Rev. Lett.* 55, 1768–1770.
- Merlin, R., Bajema, K., Nagle, J., Ploog, K., 1987. Raman scattering by acoustic phonons and structural properties of Fibonacci, Thue-morse and random superlattices. *J. Phys. Colloq.* 48 (C5), 503–506.
- Merzbacher, E., 1997. *Quantum Mechanics*, 3rd Edition. Wiley, New York.
- Mischenko, A., Fomenko, A., 1988. *A Course of Differential Geometry and Topology*. MIR, Moscow.
- Miyazawa, T., 2000. Boson representations of one-dimensional scattering. *J. Phys. A* 33, 191–225.
- Monsivais, G., García-Moliner, F., Velasco, V. R., 1995. Unified description of quantum particles and electromagnetic and elastic waves in multilayers. *J. Phys.: Condens. Matter* 7, 5491–5506.
- Monsoriu, J. A., Villatoro, F. R., Marín, M. J., Pérez, J., Monreal, L., 2006. Quantum fractal superlattices. *Am. J. Phys.* 74, 831–836.
- Monsoriu, J. A., Villatoro, F. R., Marín, M. J., Urchueguía, J. F., Fernández-Córdoba, P., 2005. A transfer matrix method for the analysis of fractal quantum potentials. *Eur. J. Phys.* 26, 603–610.
- Monzón, J. J., Barriuso, A. G., Sánchez-Soto, L. L., 2006. Perfect antireflection via negative refraction. *Phys. Lett. A* 349, 281–284.
- Monzón, J. J., Barriuso, A. G., Sánchez-Soto, L. L., 2008. Geometric picture of optical complementary media. *Eur. J. Phys.* 29, 431–437.
- Monzón, J. J., Barriuso, A. G., Sánchez-Soto, L. L., Montesinos-Amilibia, J. M., 2011. Geometrical interpretation of optical absorption. *Phys. Rev. A* 84.
- Monzón, J. J., Sánchez-Soto, L. L., 1999. Lossless multilayers and Lorentz transformations: more than an analogy. *Opt. Commun.* 162, 1–6.
- Monzón, J. J., Sánchez-Soto, L. L., 1999. Origin of the Thomas rotation that arises in lossless multilayers. *J. Opt. Soc.*

- Am. A 16, 2786–2792.
- Monzón, J. J., Sánchez-Soto, L. L., 2001. A simple optical demonstration of geometrical phases from multilayer stacks: the Wigner angle as an anholonomy. *J. Mod. Opt.* 48, 21–34.
- Monzón, J. J., Yonte, T., Sánchez-Soto, L. L., 2003. Characterizing the reflectance of periodic layered media. *Opt. Commun.* 218, 43–47.
- Monzón, J. J., Yonte, T., Sánchez-Soto, L. L., Cariñena, J. F., 2002. Geometrical setting for the classification of multilayers. *J. Opt. Soc. Am. A* 19, 985–991.
- Mora, M., Pérez-Álvarez, R., Sommers, C., 1985. Transfer matrix in one-dimensional problems. *J. Phys.* 46, 6151–6159.
- Moretti, V., 2006. The interplay of polar decomposition theorem and Lorentz group. *Lect. Notes Semin. Interdiscip. Mat.* 5, 153–170.
- Morozov, G. V., Sprung, D. W. L., Martorell, J., 2002. Design of electron band-pass filters for semiconductor superlattices. *J. Phys. D* 35, 3052–3059.
- Mugassabi, S., Vourdas, A., 2009. Almost periodic one-dimensional systems. *J. Phys. A* 42, 202001.
- Muller, R. A., 1992. Thomas precession: Where is the torque? *Am. J. Phys.* 60, 313–317.
- Nakamura, K., Shimizu, A., Koshiba, M., Hayata, K., 1989. Finite-element analysis of quantum wells of arbitrary semiconductors with arbitrary potential profiles. *IEEE J. Quantum Electron.* 25, 889–895.
- Newton, R. G., 1966. *Scattering Theory of Waves and Particles*. McGraw-Hill, New York.
- Nöckel, J. U., Stone, A. D., 1994. Resonance line shapes in quasi-one-dimensional scattering. *Phys. Rev. B* 50, 17415–17432.
- Nogami, Y., Ross, C. K., 1996. Scattering from a nonsymmetric potential in one dimension as a coupled-channel problem. *Am. J. Phys.* 64, 923–928.
- O'Donnell, K., Visser, M., 2011. Elementary analysis of the special relativistic combination of velocities, Wigner rotation and Thomas precession. *Eur. J. Phys.* 32, 1033–1047.
- Oh, G. Y., Lee, M. H., 1993. Band-structural and fourier-spectral properties of one-dimensional generalized Fibonacci lattices. *Phys. Rev. B* 48, 12465–12477.
- Olson, J. D., Mace, J. L., 2003. Wave function confinement via transfer matrix methods. *J. Math. Phys.* 44, 1596–1624.
- Ostlund, S., Pandit, R., 1984. Renormalization-group analysis of the discrete quasiperiodic Schrödinger equation. *Phys. Rev. B* 29, 1394–1414.
- Pedoe, D., 1970. *A Course of Geometry*. Cambridge University Press, Cambridge.
- Pendry, J. B., Ramakrishna, S. A., 2003. Focusing light using negative refraction. *J. Phys.: Condens. Matter* 15, 6345–6364.
- Peres, A., 1983. Transfer matrices for one-dimensional potentials. *J. Math. Phys.* 24, 1110–1119.
- Pereyra, P., 1995. Symmetries, parametrization, and group structure of transfer matrices in quantum scattering theory. *J. Math. Phys.* 36, 1166–1176.
- Pereyra, P., Castillo, E., 2002. Theory of finite periodic systems: General expressions and various simple and illustrative examples. *Phys. Rev. B* 65, 205120.
- Pérez-Álvarez, R., García-Moliner, F., 2004. Transfer matrix, Green function and related techniques. *Universitat Jaume I, Castelló*.
- Pérez-Álvarez, R., Rodríguez-Coppola, H., 1988. Transfer matrix in 1D Schrödinger problems with constant and position-dependent mass. *Phys. Stat. Sol. B*, 493–500.
- Pérez-Álvarez, R., Rodríguez-Coppola, H., Velasco, V. R., García-Moliner, F., 1988. A study of the matching problem using transfer matrices. *J. Phys. C* 21, 2197–2206.
- Pérez-Álvarez, R., Trallero-Herrero, C., García-Moliner, F., 2001. 1D transfer matrices. *Eur. J. Phys.* 22, 275–86.
- Pujol, O., Pérez, J. P., 2007. A synthetic approach to the transfer matrix method in classical and quantum physics. *Eur. J. Phys.* 28, 679–691.
- Rakityansky, S. A., 2004. Modified transfer matrix for nanostructures with arbitrary potential profile. *Phys. Rev. B* 70, 205323.
- Ram-Mohan, L. R., Yoo, K. H., Aggarwal, R. L., 1988. Transfer-matrix algorithm for the calculation of the band structure of semiconductor superlattices. *Phys. Rev. B* 38, 6151–6159.
- Ram-Mohan, R., 2002. *Finite Element and Boundary Element Applications in Quantum Mechanics*. Oxford University Press, Oxford.
- Reed, M., Simon, B., 1980. *Methods of Modern Mathematical Physics. Vol. I.- Functional Analysis*. Academic, New York.
- Rhodes, J. A., Semon, M. D., 2004. Relativistic velocity space, Wigner rotation, and Thomas precession. *Am. J. Phys.* 72, 943–960.
- Ritus, V. I., 2008. Permutation asymmetry of the relativistic velocity addition law and non-Euclidean geometry. *Phys. Usp.* 51, 709–721.
- Rodríguez-Coppola, H., Velasco, V. R., García-Moliner, F., Pérez-Álvarez, R., 1990. Transfer matrix and matrix Green function: The matching problem. *Physica Scripta* 42, 115–123.

- Rozman, M. G., Reineker, P., Tehver, R., 1994a. One-dimensional scattering: Recurrence relations and differential equations for transmission and reflection amplitudes. *Phys. Rev. A* 49, 3310–3321.
- Rozman, M. G., Reineker, P., Tehver, R., 1994b. Scattering by locally periodic one-dimensional potentials. *Phys. Lett. A* 187, 127–131.
- Salem, R., 1963. *Algebraic Numbers and Fourier Analysis*. Heath, Boston.
- Sánchez-Soto, L. L., Cariñena, J. F., Barriuso, A. G., Monzón, J. J., 2005. Vector-like representation of one-dimensional scattering. *Eur. J. Phys* 26, 469–480.
- Sassoli-de-Bianchi, M., 1994. Levinson’s theorem, zero-energy resonances, and time delay in one-dimensional scattering. *J. Math. Phys.* 35, 2719–2733.
- Sassoli-de-Bianchi, M., Ventra, M. D., 1995. On the number of states bound by one-dimensional finite periodic potentials. *J. Math. Phys.* 36, 1753–1764.
- Schutz, B. F., 1997. *Geometrical Methods of Mathematical Physics*. Cambridge University Press, Cambridge.
- Severin, M., Riklund, R., 1989. Using the Fourier spectrum to classify families of generalised extensions of the Fibonacci lattice. *J. Phys.: Condens. Matter* 1, 5607–5612.
- Shamir, J., Cohen, N., 1995. Root and power transformations in optics. *J. Opt. Soc. Am. A* 12, 2415–2423.
- Shapere, A., Wilczek, F. (Eds.), 1989. *Geometric Phases in Physics*. World Scientific, Singapore.
- Siegman, A., 1986. *Lasers*. Oxford University Press, Oxford.
- Simon, R., Chaturvedi, S., Srinivasan, V., Mukunda, N., 2006. Hamilton’s turns for the Lorentz group. *Int. J. Theo. Phys.* 45, 2075–2094.
- Simon, R., Mukunda, N., 1993a. Bargmann invariant and the geometry of the Güoy effect. *Phys. Rev. Lett.* 70, 880–883.
- Simon, R., Mukunda, N., 1993b. Twisted Gaussian Schell-model beams. *J. Opt. Soc. Am. A* 10, 95–109.
- Simon, R., Mukunda, N., 1998. Iwasawa decomposition in first-order optics: universal treatment of shape-invariant propagation for coherent and partially coherent beams. *J. Opt. Soc. Am. A* 15, 2146–2155.
- Simon, R., Mukunda, N., Sudarshan, E., 1988. Partially coherent beams and a generalized ABCD-law. *Opt. Commun.* 65, 322–328.
- Simon, R., Mukunda, N., Sudarshan, E. C. G., 1989a. Hamilton’s theory of turns generalized to  $Sp(2, R)$ . *Phys. Rev. Lett.* 62, 1331–1334.
- Simon, R., Mukunda, N., Sudarshan, E. C. G., 1989b. The theory of screws: A new geometric representation for the group  $SU(1,1)$ . *J. Math. Phys.* 30, 1000–1006.
- Simon, R., Sudarshan, E., Mukunda, N., 1985. Anisotropic Gaussian Schell-model beams: Passage through optical systems and associated invariants. *Phys. Rev. A* 31, 2419–2434.
- Simon, R., Sudarshan, E. C. G., Mukunda, N., 1984. Generalized rays in first order optics: transformation properties of Gaussian Schell-model fields. *Phys. Rev. A* 29, 3273–3279.
- Simon, R., Wolf, K., 2000. Structure of the set of paraxial optical systems. *J. Opt. Soc. Am. A* 17, 342–355.
- Singh, J., 1986. A new method for solving the ground-state problem in arbitrary quantum wells: Application to electron-hole quasi-bound levels in quantum wells under high electric field. *Appl. Phys. Lett.* 48, 434–436.
- Singh, J., 1997. *Quantum Mechanics: Fundamentals and Applications to Technology*. Wiley, New York.
- Spinadel, V. W., 1999. The metallic means family and multifractal spectra. *Nonlinear Anal.* 36, 721–745.
- Sprung, D. W. L., Morozov, G. V., Martorell, J., 2004. Geometrical approach to scattering in one dimension. *J. Phys. A* 37, 1861–1880.
- Sprung, D. W. L., Sigeitch, J. D., Jagiello, P., Martorell, J., 2003. Continuum bound states as surface states of a finite periodic system. *Phys. Rev. B* 67, 085318.
- Sprung, D. W. L., Sigeitch, J. D., Wu, H., Martorell, J., 1999. Bound states of a finite periodic potential. *Am. J. Phys.* 68, 715–722.
- Sprung, D. W. L., Wu, H., Martorell, J., 1993. Scattering by a finite periodic potential. *Am. J. Phys.* 61, 1118–1124.
- Stahl, S., 1993. *The Poincaré half-plane*. Jones and Bartlett, Boston.
- Starikov, A., Wolf, E., 1982. Coherent-mode representation of Gaussian Schell-model sources and of their radiation fields. *J. Opt. Soc. Am. A* 72, 923–928.
- Strandberg, M. W. P., 1986. Abstract group theoretical reduction of products of Lorentz-group representations. *Phys. Rev. A* 34, 2458–2461.
- Su, P., Cao, Z., Chen, K., Yin, C., Shen, Q., 2008. Explicit expression for the reflection and transmission probabilities through an arbitrary potential barrier. *J. Phys. A* 41, 465301.
- Sütö, A., 1989. Singular continuous spectrum on a Cantor set of zero Lebesgue measure for the Fibonacci Hamiltonian. *J. Stat. Phys.* 56, 525–531.
- Tamura, S., Nori, F., 1989. Transmission and frequency spectra of acoustic phonons in Thue-Morse superlattices. *Phys. Rev. B* 40, 9790–9801.
- Thomsen, J., Einevoll, G. T., Hemmer, P. C., 1989. Operator ordering in effective-mass theory. *Phys. Rev. B* 39, 12783–12788.
- Trzeciakowski, W., Gurioli, M., 1993. Density of states and transmission in the one-dimensional scattering problem. *J.*

- Phys.: Condens. Matter 5, 1701–1706.
- Tsai, Y. C., Shung, K. W., Gou, S. C., 1998. Impurity modes in one-dimensional photonic crystals: analytic approach. *J. Mod. Opt.* 45, 2147–2158.
- Tsu, R., Esaki, L., 1973. Tunneling in a finite superlattice. *Appl. Phys. Lett.* 22, 562–564.
- Ungar, A. A., 1989. The relativistic velocity composition paradox and the Thomas rotation. *Found. Phys.* 19, 1385–1396.
- Ungar, A. A., 2001. *Beyond Einstein's Velocity Addition Law*. Kluwer, Dordrecht.
- Urbantke, H., 1990. Physical holonomy, Thomas precession, and Clifford algebra. *Am. J. Phys.* 58, 747–750.
- van Dijk, W., Kiers, K. A., 1992. Time delay in simple one-dimensional systems. *Am. J. Phys.* 60, 520–527.
- Vasconcelos, M. S., Albuquerque, E. L., 1999. Transmission fingerprints in quasiperiodic dielectric multilayers. *Phys. Rev. B* 59, 11128–11131.
- Velasco, V. R., García-Moliner, F., 2003. Electronic spectra of quasi-regular heterostructures: simple versus realistic models. *Prog. Surf. Sci.* 74, 343–355.
- Veselago, V. G., 1968. The electrodynamics of substances with simultaneously negative values of  $\epsilon$  and  $\mu$ . *Sov. Phys. Usp.* 10, 509–514.
- Vezezzetti, D. J., Cahay, M., 1986. Transmission resonances in finited repeated structures. *J. Phys. D* 19, L53–55.
- Vigoureux, J. M., 1992. Use of Einstein's addition law in studies of reflection by stratified planar structures. *J. Opt. Soc. Am. A* 9, 1313–1319.
- Vigoureux, J. M., Grossel, P., 1993. A relativistic-like presentation of optics in stratified planar media. *Am. J. Phys.* 61, 707–712.
- Vinter, B., Weisbuch, C., 1991. *Quantum Semiconductor Structures*. Academic, New York.
- Visser, M., 1999. Some general bounds for one-dimensional scattering. *Phys. Rev. A* 59, 427–438.
- Walker, J. S., Gathright, J., 1994. Exploring one-dimensional quantum mechanics with transfer matrices. *Am. J. Phys.* 62, 408–422.
- Weber, T. A., 1994. Bound states with no classical turning points in semiconductor heterostructures. *Solid State Comm.* 90, 713–716.
- Wen, Y., Cheng, Y., Xian-Ping, W., Zhuang-Qi, C., 2010. Quantum reflection as the reflection of subwaves. *Chin. Phys. B* 19, 093402.
- Wolf, E., Collett, E., 1978. Partially coherent sources which produce the same far-field intensity distribution as a laser. *Opt. Commun* 25, 293–296.
- Wolf, K. B., 2004. *Geometric Optics on Phase Space*. Springer, Berlin.
- Wu, H., Sprung, D. W. L., Martorell, J., 1993. Periodic quantum wires and their quasi-one- dimensional nature. *J. Phys. D* 26, 798–803.
- Wybourne, B. G., 1974. *Classical Groups for Physicists*. Wiley, New York.
- Wyk, C. B. V., 1984. Rotation associated with the product of two Lorentz transformations. *Am. J. Phys.* 52, 853–854.
- Xuereb, A., Domokos, P., Asbóth, J., Horak, P., Freearge, T., 2009. Scattering theory of cooling and heating in optomechanical systems. *Phys. Rev. A* 79, 053810.
- Yeh, P., 1988. *Optical Waves in Layered Media*. Wiley, New York.
- Yonte, T., Monzón, J. J., Sánchez-Soto, L. L., Cariñena, J. F., López-Lacasta, C., 2002. Understanding multilayers from a geometrical viewpoint. *J. Opt. Soc. Am. A* 19, 603–609.
- Yuan, W., Yin, C., Wang, X.-P., Cao, Z.-Q., 2010. Quantum reflection as the reflection of subwaves. *Chin. Phys. B* 19, 093402.
- Zárate, J. E., Velasco, V. R., 2001. Electronic properties of quasiperiodic heterostructures. *Phys. Rev. B* 65, 045304.
- Zel'dovich, B. Y., Pilipetsky, N. F., Shkunov, V. V., 1985. *Principles of Phase Conjugation*. Springer, Berlin.
- Zieschang, H., Vogt, E., Coldewey, H.-D., 1980. Surfaces and planar discontinuous groups. Vol. 835 of *Lecture Notes in Mathematics*. Springer, Berlin.